MANCHESTER
1824

The University
of Manchester

Point Vortices on the Sphere: Stability of Symmetric Relative Equilibria

Laurent-Polz, Frederic and Montaldi,
James and Roberts, Mark

2011

MIMS EPrint: **2005.28**

Manchester Institute for Mathematical Sciences
School of Mathematics

The University of Manchester

Reports available from: http://eprints.maths.manchester.ac.uk/
And by contacting: The MIMS Secretary
School of Mathematics
The University of Manchester
Manchester, M13 9PL, UK

ISSN 1749-9097

JOURNAL OF GEOMETRIC MECHANICS
©American Institute of Mathematical Sciences
Volume **3**, Number **4**, December **2011**
doi:10.3934/jgm.2011.3.439
pp. **439–486**

POINT VORTICES ON THE SPHERE: STABILITY OF SYMMETRIC RELATIVE EQUILIBRIA

Frederic Laurent-Polz

Institut Non Linéaire de Nice
1361 route des Lucioles
06560 Valbonne, France

James Montaldi

School of Mathematics
University of Manchester
Manchester, M13 9PL, UK

Mark Roberts

Department of Mathematics
University of Surrey
Guildford GU2 7XH, UK

Dedicated to Tudor Ratiu on the occasion of his 60th birthday

Abstract. We describe the linear and nonlinear stability and instability of certain symmetric configurations of point vortices on the sphere forming relative equilibria. These configurations consist of one or two rings, and a ring with one or two polar vortices. Such configurations have dihedral symmetry, and the symmetry is used to block diagonalize the relevant matrices, to distinguish the subspaces on which their eigenvalues need to be calculated, and also to describe the bifurcations that occur as eigenvalues pass through zero.

Contents

1. Introduction 440
2. Point vortices on the sphere and stability theory 444
3. Symmetry adapted bases for rings and poles 446
4. Bifurcations and symmetry 450
5. A ring of identical vortices: $\mathbf{C}_{nv}(R)$ 453
6. A ring with a polar vortex: $\mathbf{C}_{nv}(R,p)$ 459
7. Two aligned rings: $\mathbf{C}_{nv}(2R)$ 467
8. Two staggered rings: $\mathbf{C}_{nv}(R,R')$ 471
9. A ring with two polar vortices: $\mathbf{C}_{nv}(R,2p)$ 475
REFERENCES 484

2000 *Mathematics Subject Classification.* Primary: 37J15, 37J20, 37J25, 70H33, 76B47.
Key words and phrases. Point vortices, Hamiltonian systems, stability, bifurcations, symmetry.

1. **Introduction.** Since the work of Helmholtz [10], and later Kirchhoff [13], systems of point vortices on the plane have been studied as finite-dimensional approximations to vorticity dynamics in ideal fluids. For a general survey of patterns of point vortices see Aref *et al* [1]. Point vortex systems on the sphere, introduced by Bogomolov [2], provide simple models for the dynamics of concentrated regions of vorticity, such as cyclones and hurricanes, in planetary atmospheres. In this paper we consider a non-rotating sphere, since the rotation of the sphere induces a non-uniform background vorticity which makes the whole system infinite-dimensional.

As in the planar case, the equations governing the motion of N point vortices on a sphere are Hamiltonian [2] and this property has been used to study them from a number of different viewpoints. Phase space reduction shows that the three vortex problem is completely integrable on both the plane and the sphere: the motion of three vortices of arbitrary vorticity on a sphere is studied in [12]. The stability of some of the relative equilibria described in [12] are computed in [39] and numerical simulations are presented in [20]. The existence of relative equilibria of N vortices is treated in [19], and the nonlinear stability of a latitudinal ring of N identical vorticities is computed in [3], and independently in the present paper. In fact the linear stability results of such a ring obtained in [38] coincide with the Lyapounov stability results. The stability of a ring of vortices on the sphere together with a central polar vortex is studied in [5], and again independently in the present paper, though with different methods (and stronger results). The existence and nonlinear stability of relative equilibria of N vortices of vorticity $+1$ together with N vortices of vorticity -1 are studied in [15]. It has also been proved in [17] that relative equilibria formed of latitudinal rings of identical vortices for the non-rotating sphere persist to relative equilibria when the sphere rotates. However, the question of stability becomes much more delicate: for motions that are not relative equilibria, the vorticity of a point vortex is no longer preserved as it interacts with the background vorticity, and the problem becomes fundamentally infinite-dimensional. In [14] Kurakin studies the stability of equilibrium configurations of identical vortices placed at the vertices of regular polyhedra; he finds that the tetrahedron, octahedron and icosahedron are stable, while the other two are unstable. Finally, studies of periodic orbits of point vortices on the sphere can be found in [41, 42, 18, 16].

Our study of the stability of relative equilibria is based on the symmetries of the system, and especially the isotropy subgroups of the relative equilibria. The Hamiltonian is invariant under rotations and reflexions of the sphere and permutations of identical vortices. However, some of these symmetries (eg reflexions) are not symmetries of the equations of motion: they are *time-reversing* symmetries. From Noether's theorem, the rotational symmetry provides three conserved quantities, the components of the momentum map $\Phi : \mathcal{P} \to \mathbb{R}^3$ where $\mathcal{P}$ is the phase space.

Relative equilibria (RE) are dynamical trajectories that are generated by the action of a 1-parameter subgroup of the symmetry group. More intuitively, they correspond here to motions of the point vortices which are stationary in a steadily rotating frame. In other words, the motion of a relative equilibrium corresponds to a rigid rotation of N point vortices about some axis (which we always take to be the z-axis). In the same way as equilibria are critical points of the Hamiltonian H, relative equilibria are critical points of the restrictions of H to the level sets of Φ. Section 2 is devoted to a description of the system of point vortices on the sphere, and to an outline of stability theory for relative equilibria. The appropriate concept of stability for relative equilibria of Hamiltonian system is Lyapounov stability *modulo*

a subgroup. The stability study is realized using on one hand the *energy-momentum method* [36, 34] which consists of computing the eigenvalues of a certain Hessian, and leads to *nonlinear* stability results, and on the other hand a linear study computing the eigenvalues of the linearization of the equations of motion. To both these ends, we block diagonalize these matrices using a suitable basis, the *symmetry adapted basis* (Section 3), which makes use of the specific dihedral symmetry of the relative equilibrium. This is equivalent to noting that the matrices (or certain submatrices) are *circulant*, as used in [5]. The symmetry adapted basis splits the tangent space to the phase space into a number of modes, from $\ell = 0$ to $\ell = [n/2]$ (where n is the number of vortices in the ring), and calculations can proceed separately for each mode. Moreover, the symmetry is also used to apply the energy-momentum method as it helps distinguish on which subspaces computations are needed. In Section 4 we outline the different bifurcations which occur in this system: symmetric pitchforks, Hamiltonian Hopf bifurcations and those bifurcations which occur due to the 'geometry of reduction'—those occurring in a neighbourhood of points with zero momentum.

The remaining five sections each treat one of five different types of relative equilibrium, consisting of rings of identical vortices together with possible vortices at the poles, whose existence were proved in [19]. The notation for the different configurations is taken from the same source and is described at the end of the introduction. We now outline the main stability results.

We begin in Section 5 by computing the stability of the relative equilibria consisting of a single ring of identical vortices, a configuration denoted $\mathbf{C}_{nv}(R)$ (Figure 1.1(a)). We show in Theorem 5.2 that for $n \geq 7$, they are unstable for all co-latitudes[1] of the ring, while for $n < 7$ there exist ranges of Lyapounov stability when the ring is near a pole. These results are not new [38] (for linear stability results) and [3] (for nonlinear stability), but serve to demonstrate the method used in later sections.

In Section 6, we study the stability of the relative equilibria $\mathbf{C}_{nv}(R, p)$ (Figure 1.1(b)) which are configurations formed of a ring of n identical vortices together with a single polar vortex. For $n \geq 7$ they are all unstable if the vorticity κ of the polar vortex has opposite sign to that of the ring. However if the vorticities have the same sign then for each co-latitude of the ring there exists a range of κ for which the relative equilibrium is Lyapounov stable. Adding polar vortices can therefore *stabilize* the unstable pure ring relative equilibria. The detailed results are contained in Theorem 6.2, its corollary and the following discussion. Our results are consistent with those of [5] (aside from an error in their Figure 7 where the wrong curves are plotted), though the present methods are stronger as they give more regions of stability than obtained in [5]—see Remark 6.4.

In Sections 7 and 8 we investigate configurations formed of two rings of arbitrary vorticities (each ring, as always, consisting of identical vortices). In [19] it was shown that two rings of n vortices can be relative equilibria if and only if they are either aligned or staggered. These two arrangements are denoted $\mathbf{C}_{nv}(2R)$ and $\mathbf{C}_{nv}(R, R')$ respectively (see Figure 1.2). Here we show that for almost all pairs of ring latitudes there is a unique ratio of the ring vorticities for which these configurations are relative equilibria. Numerical computations of their stability suggest that these relative equilibria can only be stable if $n \leq 6$, and in the aligned case the two rings

[1] the co-latitude θ of a point on the sphere is the angle subtended with the North pole

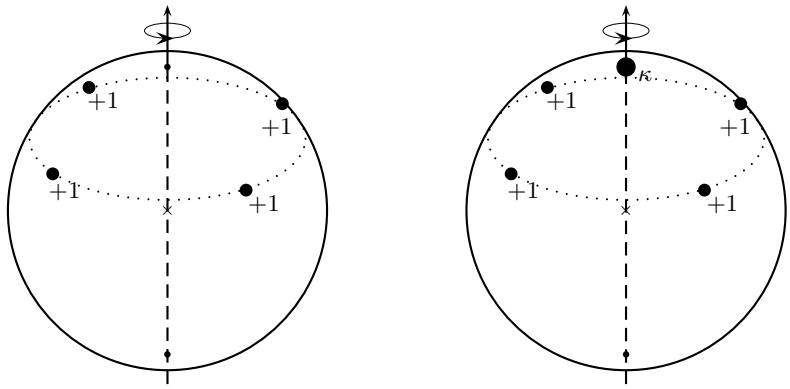

FIGURE 1.1. The $\mathbf{C}_{nv}(R)$ and $\mathbf{C}_{nv}(R,p)$ relative equilibria, here shown for $n=4$. The $\mathbf{C}_{nv}(R,2p)$ configurations have a vortex at the South pole as well.

must be close to opposite poles, and hence have opposite vorticities. In some cases, staggered rings may also be stable when in the same hemisphere.

Finally, in Section 9 we study the relative equilibria $\mathbf{C}_{nv}(R,2p)$ which are configurations formed of a ring of n identical vortices together with *two* polar vortices. The two polar vorticities make this a 2-parameter family of systems. We obtain analytic (in)stability criteria, but only with respect to certain modes ($\ell \geq 2$). As in the case of a single polar vortex, the two polar vortices play the role of control parameters for the stability. The details are contained in Theorem 9.2. We then continue with numerical investigations for the remaining mode ($\ell = 1$) in order to provide full stability criteria; the conclusions are shown in a series of stability diagrams. Further diagrams are available on the second author's website [27].

The numerical computations all consist simply of computing the eigenvalues of the Hessian of the Hamiltonian and the linear vector field on the symplectic slice, using the block diagonalization of the matrices to simplify the calculations. These are precisely the same calculations as in the earlier sections where they can be performed analytically. The numerics are all done using MAPLE, and a selection of the code can also be downloaded from [27].

In principle the method applies to larger numbers of rings but the algebraic problem of diagonalizing the matrices in general becomes intractable; however numerical studies for particular (numerical) values of the vorticities in the rings would be feasible.

Symmetry group notation All possible symmetry types of configurations of point vortices on the sphere were classified in [19]. The symmetry group of the system is of the form $\mathsf{O}(3) \times S$, where S is a group of permutations, and a particular configuration with symmetry, or isotropy, subgroup $\Sigma < \mathsf{O}(3) \times S$ is denoted $\Gamma(A)$, where Γ is the projection of Σ to $\mathsf{O}(3)$ and A represents the way Σ permutes the point vortices, so describing their geometry (for example $A = R$ means they are in a ring, $A = p$ means a polar vortex). The classical *Schönflies-Eyring* notation for subgroups of $\mathsf{O}(3)$ is used.

In this paper we single out configurations consisting of concentric rings of identical vortices, with the same number of vortices in each ring, and with possible polar

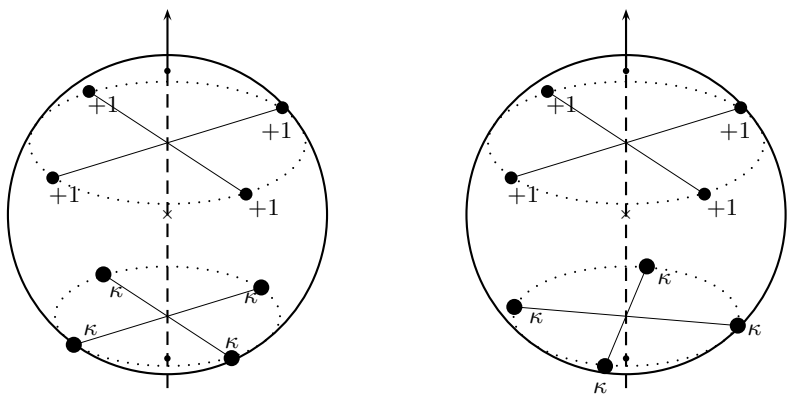

FIGURE 1.2. Configurations of types $\mathbf{C}_{nv}(2R)$ (2 aligned rings) and $\mathbf{C}_{nv}(R, R')$ (2 staggered rings). As in the previous figure, this is depicted for $n = 4$.

vortices. These configurations have cyclic symmetry (in the 'horizontal plane'), and the Schönflies-Eyring notation for this subgroup of $\mathsf{O}(3)$ is $\mathbf{C}_n < \mathsf{SO}(3)$. In fact we only consider the cases where the rings are either aligned (the vortices lie on the same longitudes) or staggered (they lie on intermediate longitudes, out of phase by π/n). In these two cases the symmetry group is the larger *dihedral* group $\mathbf{C}_{nv}$ (n being the number of vortices in each ring, and v denoting the fact that there are vertical planes of reflexion). For such configurations, we write $\mathbf{C}_{nv}(k_1R, k_2R', k_pp)$ to mean that there are $k_r = k_1 + k_2$ rings and k_p polar vortices. The difference between R and R' is that the k_1 rings R are all aligned and the k_2 rings R' are staggered with respect to the first (and so aligned with each other). Of course $k_p = 0, 1$ or 2.

In particular, the following table shows the five types of configuration we consider in detail and the relevant section in this paper:

$\mathbf{C}_{nv}(R)$	a single ring of n identical vortices	§ 5
$\mathbf{C}_{nv}(R, p)$	a single ring as above, together with a polar vortex	§ 6
$\mathbf{C}_{nv}(2R)$	a pair of aligned rings of n identical vortices	§ 7
$\mathbf{C}_{nv}(R, R')$	a pair of staggered rings of n identical vortices	§ 8
$\mathbf{C}_{nv}(R, 2p)$	a single ring as above, together with two polar vortices	§ 9

We also refer on occasion to other symmetry types. In particular $\mathbf{D}_{nh}$ is the subgroup of $\mathsf{O}(3)$ generated by the dihedral group $\mathbf{C}_{nv}$ together with a reflexion in the horizontal plane: it is the symmetry group of a pair of aligned rings of vortices lying symmetrically about the equator. Similarly, $\mathbf{D}_{nd}$ is the subgroup generated by $\mathbf{C}_{nv}$ together with a combined reflexion-rotation: reflexion about the horizontal plane combined with a rotation by π/n (the rotations in $\mathbf{C}_{nv}$ are through multiples of $2\pi/n$). This is the symmetry group of a pair of staggered rings of vortices lying at opposite latitudes.

For the symmetry arguments to hold, the vortices in a single ring must be identical, but we do not assume that the vortices in different rings or at the poles are identical.

Historical note An early version of this paper was written in 2002, with most of the stability calculations performed by the first author (FLP). It was submitted soon after, but the editor asked for more extensive numerics. This lay in the to-do pile of the other two authors for the intervening years (FLP having left academic research in the meantime), and the occasion of Tudor Ratiu's birthday celebration was the impetus required to produce a final version, with the more extensive numerics—especially those in the final section.

2. **Point vortices on the sphere and stability theory.** In this section we briefly recall that the system of point vortices on a sphere is an n-body Hamiltonian system with symmetry and we review the stability theory for relative equilibria.

2.1. **Point vortices.** Consider n point vortices $x_1, \dots, x_n \in S^2$ with vorticities $\kappa_1, \dots, \kappa_n \in \mathbb{R}$. Let θ_i, ϕ_i be respectively the co-latitude and the longitude of the vortex x_i (so $\theta = 0$ corresponds to the North pole). The dynamical system is Hamiltonian with Hamiltonian given by

$$H \;=\; -\sum_{i<j} \kappa_i \kappa_j \ln(1 - \cos\theta_i \cos\theta_j - \sin\theta_i \sin\theta_j \cos(\phi_i - \phi_j))$$

and conjugate variables given by $q_i = \sqrt{|\kappa_i|}\cos\theta_i$ and $p_i = \operatorname{sign}(\kappa_i)\sqrt{|\kappa_i|}\phi_i$. Note that many authors have a constant factor (involving π) in the Hamiltonian; this will not effect the existence or stability of the relative equilibria, but is equivalent to a rescaling of time by that factor.

The phase space is $\mathcal{P} = \{(x_1, \dots, x_n) \in S^2 \times \cdots \times S^2 \mid x_i \neq x_j \text{ if } i \neq j\}$ endowed with the symplectic form $\omega = \sum_i \kappa_i \sin\theta_i \; d\theta_i \wedge d\phi_i$. The Hamiltonian vector field X_H satisfies $\omega(\,\cdot\,, X_H(x)) = dH_x$. If we consider S^2 as a subset of $\mathbb{R}^3$, so each vortex $x_j \in \mathbb{R}^3$, then we obtain

$$\begin{aligned} \dot{x_i} \;&=\; X_H(x)_i \;=\; \sum_{j, j\neq i} \kappa_j \, \frac{x_j \times x_i}{1 - x_i \cdot x_j} \;,\; i = 1, \dots, N, \\ H \;&=\; -\sum_{i<j} \kappa_i \kappa_j \ln(\|x_i - x_j\|^2/2). \end{aligned} \tag{2.1}$$

It follows that H is invariant under $\mathsf{O}(3)$ acting by rotations and reflexions of the sphere.

The rotation subgroup $\mathsf{SO}(3)$ leaves the symplectic form invariant, and so the Hamiltonian vector field X_H is $\mathsf{SO}(3)$-equivariant. On the other hand, the reflexions in $\mathsf{O}(3)$ reverse the sign of the symplectic form and so give rise to time-reversing symmetries of X_H. Moreover H, ω and X_H are all invariant (or equivariant) with respect to permutations of vortices with equal vorticity.

The rotational symmetry implies the existence of a momentum map $\Phi : \mathcal{P} \to \mathfrak{so}(3)^* \simeq \mathbb{R}^3$:

$$\Phi(x) \;=\; \sum_{j=1}^{N} \kappa_j x_j \qquad (x_j \in S^2 \subset \mathbb{R}^3) \tag{2.2}$$

which is conserved under the dynamics. In other words each of the three components of $\Phi(x)$ is a conserved quantity. We will always orient the solution we are studying so that $\Phi(x)$ lies on the z-axis, and write $\Phi(x) = (0, 0, \mu)$. There is no intrinsic difference between $\mu > 0$ and $\mu < 0$—they are rotationally equivalent. However when studying bifurcations in a neighbourhood of a point with $\mu = 0$, then the two sides should be distinguished.

2.2. **Relative equilibria.** A point $x_e \in \mathcal{P}$ is a relative equilibrium if and only if there exists $\xi \in \mathfrak{so}(3) \simeq \mathbb{R}^3$ (the angular velocity) such that x_e is a critical point of the function $H_\xi(x) = H(x) - \langle \Phi(x), \xi \rangle$, where the pairing $\langle\ ,\ \rangle$ between $\mathbb{R}^3$ and its dual is identified with the canonical scalar product on $\mathbb{R}^3$. Equivalently, relative equilibria are critical points of the restriction of H to $\Phi^{-1}(\mu)$, since the level set $\Phi^{-1}(\mu)$ are always non-singular for point vortex systems of more than two vortices. The function H_ξ is called the *augmented Hamiltonian*.

Since the momentum is conserved, we can choose a frame for $\mathbb{R}^3$ such that Φ is parallel to the z-axis (provided the momentum is non-zero). It follows from the symmetry that the angular velocity $\xi \in \mathbb{R}^3$ is also parallel to the z-axis. We can therefore identify ξ and Φ with their z-components and the augmented Hamiltonian becomes simply $H_\xi(x) = H(x) - \xi\Phi(x)$.

Let $f : \mathcal{P} \to \mathbb{R}$ be a K-invariant function with K a compact group. Recall that $\mathrm{Fix}(K) = \{x \in \mathcal{P} \mid g \cdot x = x,\ \forall g \in K\}$. The *Principle of Symmetric Criticality* [35] states that a critical point of the restriction of a K-invariant function f to $\mathrm{Fix}(K)$ is a critical point of f. As a corollary, if the Hamiltonian is invariant under K and x_e is an isolated point in $\mathrm{Fix}(K) \cap \Phi^{-1}(\mu)$, then x_e is a relative equilibrium. It follows in particular that all configurations of type $\mathbf{C}_{nv}(R)$, $\mathbf{C}_{nv}(R,p)$ (Figure 1.1), and $\mathbf{C}_{nv}(R,2p)$ are relative equilibria: take K such that $\pi(K) = \mathbf{C}_{nv}$ where $\pi : \mathsf{O}(3) \times S_n \to \mathsf{O}(3)$ is the Cartesian projection.

Finally, one can show that if x_e is a relative equilibrium with angular velocity ξ, then H_ξ is a G_{x_e}-invariant function, where $G_{x_e} < \mathsf{O}(3) \times S$ is the symmetry group (isotropy group) of the configuration x_e.

2.3. **Stability theory and isotypic decomposition.** Stability is determined by the energy-momentum method together with an isotypic decomposition of the symplectic slice. We recall the main points of the method.

Let $x_e \in \mathcal{P}$ be a relative equilibrium, $\mu = \Phi(x_e)$, and ξ be its angular velocity. The energy-momentum method consists of determining the symplectic slice

$$\mathcal{N} \ = \ (\mathfrak{so}(3)_\mu \cdot x_e)^\perp \cap \mathrm{Ker}\, D\Phi(x_e)$$

transverse to $\mathfrak{so}(3)_\mu \cdot x_e$, where

$$\mathsf{SO}(3)_\mu \ = \ \{g \in \mathsf{SO}(3) \mid \mathrm{Coad}_g \cdot \mu = \mu\}$$

and then examining the definiteness of the restriction $\mathsf{d}^2 H_\xi|_{\mathcal{N}}(x_e)$ of the Hessian $\mathsf{d}^2 H_\xi(x_e)$ to $\mathcal{N}$. (In practice we will represent μ as a vector, in which case $\mathrm{Coad}_g\, \mu = g\mu$ is just matrix multiplication.) If K is a group acting on the phase space a relative equilibrium x_e is said to be *Lyapounov stable modulo* K if for all K-invariant open neighbourhoods V of $K \cdot x_e$ there is an open neighbourhood $U \subseteq V$ of x_e which is invariant under the Hamiltonian dynamics. The *energy-momentum theorem* of Patrick [36] holds since $\mathsf{SO}(3)$ is compact, and so we have:

If $\mathsf{d}^2 H_\xi|_{\mathcal{N}}(x_e)$ is definite, then x_e is Lyapounov stable modulo $\mathsf{SO}(3)_\mu$.

For $\mu \neq 0$, $\mathsf{SO}(3)_\mu$ is the set of rotations with axis $\langle \mu \rangle$, and so isomorphic to $\mathsf{SO}(2)$, while for $\mu = 0$, $\mathsf{SO}(3)_\mu = \mathsf{SO}(3)$. If $\mu \neq 0$ Lyapounov stability modulo $\mathsf{SO}(3)_\mu$ of a relative equilibrium with non-zero angular velocity coincides with ordinary (orbital) stability of the corresponding periodic orbit.

The second ingredient consists of performing an isotypic decomposition of the symplectic slice $\mathcal{N}$ in order to block diagonalize $\mathsf{d}^2 H_\xi|_{\mathcal{N}}(x_e)$. Let V be a finite dimensional representation of a compact Lie group K. Recall that a K invariant subspace $W \subset V$ of K is said to be *irreducible* if W has no proper K invariant

subspaces. Since K is compact, V can be expressed as a direct sum of irreducible representations: $V = W_1 \oplus \cdots \oplus W_n$. In general this is not unique. There are a finite number of isomorphism classes of irreducible representations of K in V, say $U_1, \ldots, U_\ell$. Let V_k $(k = 1, \ldots, \ell)$ be the sum of all those irreducible representations W_j in the above sum for which W_j is isomorphic to U_k. Then $V = V_1 \oplus \cdots \oplus V_\ell$. This decomposition of V is unique and is called the *K-isotypic decomposition* of V [40]. By Schur's Lemma, the matrix of a K-equivariant linear map $f : V \to V$ block diagonalizes with respect to a basis $\mathcal{B} = \{\mathcal{B}_1, \ldots, \mathcal{B}_l\}$ where $\mathcal{B}_k$ is a basis of V_k, each block corresponding to a subspace V_k. The basis $\mathcal{B}$ is called a *symmetry adapted basis*. In this paper, the isotropy group K is a dihedral group, and the corresponding symmetry adapted basis consists of 'Fourier modes', defined below.

Let G denote the group of all symmetries of the Hamiltonian H and vector field X_H and G^0 the subgroup consisting of time-preserving symmetries, i.e. those acting symplectically. The elements of $G \setminus G^0$ reverse the symplectic form, and hence reverse the vector field X_H, so effectively reversing time. In the case of N identical vortices we have $G = \mathsf{O}(3) \times S_N$ and $G^0 = \mathsf{SO}(3) \times S_N$. Since H_ξ is a G_{x_e}-invariant function, the restricted Hessian $\mathsf{d}^2 H_\xi|_{\mathcal{N}}(x_e)$ is G_{x_e}-equivariant as a matrix. Moreover the symplectic slice $\mathcal{N}$ is a G_{x_e}-invariant subspace and so we can implement a G_{x_e}-isotypic decomposition of $\mathcal{N}$ to block diagonalize $\mathsf{d}^2 H_\xi|_{\mathcal{N}}(x_e)$. This block diagonalization of $\mathsf{d}^2 H_\xi|_{\mathcal{N}}(x_e)$ simplifies the computation of its eigenvalues, and hence of its definiteness. If it is definite then the relative equilibrium is Lyapounov stability modulo $\mathsf{SO}(3)_\mu$.

If $\mathsf{d}^2 H_\xi|_{\mathcal{N}}(x_e)$ is *not* definite then we study the spectral stability of x_e. In particular we examine the eigenvalues of $L_{\mathcal{N}}$, the matrix of the linearized system on the symplectic slice, that is $L_{\mathcal{N}} = \mathbf{J}_{\mathcal{N}} \, \mathsf{d}^2 H_\xi|_{\mathcal{N}}(x_e)$, where $\mathbf{J}_{\mathcal{N}}^{-1}$ is the matrix of $\omega|_{\mathcal{N}}$. The matrix $L_{\mathcal{N}}$ is $G^0_{x_e}$-equivariant and so we perform a $G^0_{x_e}$-isotypic decomposition of $\mathcal{N}$ to obtain a block diagonalization of $L_{\mathcal{N}}$, and so to determine the spectral stability of x_e. In particular, if $L_{\mathcal{N}}$ has eigenvalues with non-zero real part, then x_e is linearly unstable. Note that the block diagonalization of $\mathsf{d}^2 H_\xi|_{\mathcal{N}}(x_e)$ refines that of $L_{\mathcal{N}}$ since $G^0_{x_e} \subset G_{x_e}$.

Throughout this paper, we will align the vortices so that $\phi(x_e)$ lies along the z-axis, and we write $\phi(x_e) = (0, 0, \mu)$. If $\mu \neq 0$ then *Lyapounov stable* will mean *Lyapounov stable modulo* $\mathsf{SO}(2)$, while if $\mu = 0$ it means *Lyapounov stable modulo* $\mathsf{SO}(3)$.

3. **Symmetry adapted bases for rings and poles.** In this section we give the ingredients needed to determine the symmetry adapted bases for the symplectic slice at the configurations described above, that is those of type $\mathbf{C}_{nv}(k_1 R, k_2 R', k_p p)$. In the first subsection we give a general symmetry adapted basis for the tangent space $T_{x_e}\mathcal{P}$ to the phase space at such a configuration, and express the derivative of the momentum map and tangent space to the group orbit in this basis. In the following two subsections we describe the isotypic decomposition of $T_{x_e}\mathcal{P}$, first for a single ring and then in general. Recall that the isotropy subgroup G_{x_e} is always a dihedral group $\mathbf{C}_{nv}$ (which has order $2n$) and that the irreducible representations of this group are of dimension 1 or 2. The cyclic subgroup $\mathbf{C}_n$ acts symplectically and is denoted $G^0_{x_e}$.

The actual symmetry adapted bases of the symplectic slices will be given case-by-case in the following sections. We do not give the proof of the results in the first

subsection, since they can be easily deduced from the proofs of Propositions 4.1–4.4 in [15].

3.1. **Description of the symplectic slice.** Let x_e be a $\mathbf{C}_{nv}(k_1R, k_2R', k_pp)$ configuration. Let $k_r = k_1 + k_2$ be the total number of rings. The total number of vortices is then $N = nk_r + k_p$, where $k_p = 0, 1$ or 2 is the number of polar vortices. We suppose the vorticities in ring j are κ_j for $j = 1, \ldots, k_r$ while the vorticities of the possible polar vortices are κ_N for the North pole and κ_S for the South pole. In this paper we only consider in detail $k_r = 1$ or 2, but here we describe the more general case.

For each ring $j = 1, \ldots, k_r$ let $s = 1, \ldots, n$ label the vortices in the ring in cyclic order (in an easterly direction), and define *real* tangent vectors $\alpha^{(\ell)}_{j,\theta}$ etc. in $T_{x_e}\mathcal{P}$ by

$$\begin{aligned} \alpha^{(\ell)}_{j,\theta} + \mathsf{i}\,\beta^{(\ell)}_{j,\theta} &= \textstyle\sum_{s=1}^{n} \mathsf{e}^{\mathsf{i}\ell\phi_{j,s}}\,\delta\theta_{j,s} \\ \alpha^{(\ell)}_{j,\phi} + \mathsf{i}\,\beta^{(\ell)}_{j,\phi} &= \textstyle\sum_{s=1}^{n} \mathsf{e}^{\mathsf{i}\ell\phi_{j,s}}\,\delta\phi_{j,s} \end{aligned} \tag{3.1}$$

where $\ell = 0, \ldots, [n/2]$, $\mathsf{i} = \sqrt{-1}$ and $\phi_{j,s} = 2\pi s/n - \phi^0_j$, which is the longitude of the sth vortex in ring j, where $\phi^0_j = 0$ or π/n depending on whether the jth ring of vortices is of type R or R'. Note that $\beta^{(\ell)}_{j,\theta}, \beta^{(\ell)}_{j,\phi}$ vanish for $\ell = 0$ and $n/2$ (for n even). The vectors $\alpha^{(\ell)}_{j,\theta}$ etc. defined in (3.1) are called the *Fourier modes*, and are depicted (for $n = 4$ and 5 and rings of type R) in Figure 9.6 at the end of the paper.

For each pole $i = 1, \ldots, k_p$ (where $k_p = 0, 1, 2$) we also have tangent vectors δx_i and δy_i.

The tangent vectors defined in the last two paragraphs are almost canonical, in the sense that

$$\begin{aligned} \omega\left(\alpha^{(\ell)}_{j,\theta},\, \alpha^{(\ell)}_{j,\phi}\right) &= \begin{cases} n\sin\theta_j\,\kappa_j & \text{if } \ell = 0,\, n/2 \\ \frac{1}{2}n\,\sin\theta_j\,\kappa_j & \text{otherwise} \end{cases} \\ \omega\left(\beta^{(\ell)}_{j,\theta},\, \beta^{(\ell)}_{j,\phi}\right) &= \tfrac{1}{2}n\sin\theta_j\,\kappa_j \\ \omega\left(\delta x_i,\, \delta y_i\right) &= \operatorname{sign}(z_i)\,\kappa_i, \end{aligned} \tag{3.2}$$

while all other pairings vanish.

The cyclic subgroup $\mathbf{C}_n$ of the isotropy subgroup $\mathbf{C}_{nv} < \mathsf{O}(3) \times S$ (see the end of the Introduction) acts symplectically, and in terms of the Fourier modes, the action of the generator $\sigma \in \mathbf{C}_n$ is

$$\begin{aligned} \sigma \cdot (\alpha^{(\ell)}_{j,\theta} + \mathsf{i}\beta^{(\ell)}_{j,\theta}) &= \exp\left(\tfrac{2\pi\mathsf{i}\ell}{n}\right)(\alpha^{(\ell)}_{j,\theta} + \mathsf{i}\beta^{(\ell)}_{j,\theta}) \\ \sigma \cdot (\alpha^{(\ell)}_{j,\phi} + \mathsf{i}\beta^{(\ell)}_{j,\phi}) &= \exp\left(\tfrac{2\pi\mathsf{i}\ell}{n}\right)(\alpha^{(\ell)}_{j,\phi} + \mathsf{i}\beta^{(\ell)}_{j,\phi}) \\ \sigma \cdot (\delta x_j + \mathsf{i}\delta y_j) &= \exp\left(\tfrac{2\pi\mathsf{i}}{n}\right)(\delta x_j + \mathsf{i}\delta y_j). \end{aligned} \tag{3.3}$$

The reflexions in $\mathbf{C}_{nv} \simeq \mathbf{D}_n$ (dihedral group) act antisymplectically. One of the reflexions $\kappa \in \mathbf{D}_n \setminus \mathbf{C}_n$ acts on the sphere by $(\theta,\, \phi) \mapsto (\theta,\, -\phi)$ and by permuting the particles within each ring by,

$$\kappa \cdot (1, \ldots, n) = \begin{cases} (n-1, \ldots, 1, n) & \text{for rings of type } R, \\ (n, \ldots, 2, 1) & \text{for rings of type } R'. \end{cases}$$

The difference arises because for rings of type R, vortex n lies in the half-plane $\phi = 0$, while for rings of type R' it lies in the half-plane $\phi = -\pi/n$. In terms of the

Fourier modes, this reflexion acts by,

$$\begin{aligned} &\alpha^{(\ell)}_{j,\theta} \mapsto \alpha^{(\ell)}_{j,\theta}\,, && \beta^{(\ell)}_{j,\theta} \mapsto -\beta^{(\ell)}_{j,\theta}\,, \\ &\beta^{(\ell)}_{j,\phi} \mapsto \beta^{(\ell)}_{j,\phi}\,, && \alpha^{(\ell)}_{j,\phi} \mapsto -\alpha^{(\ell)}_{j,\phi}, \\ &\delta x \mapsto \delta x\,, && \delta y \mapsto -\delta y\,. \end{aligned}$$

Each of the subspaces $\left\langle \alpha^{(\ell)}_{j,\theta},\, \beta^{(\ell)}_{j,\theta} \right\rangle$ and similarly with ϕ are $\mathbf{D}_n$-invariant isotropic subspaces.

In order to compute a specific basis for the symplectic slice it is necessary to have expressions for the derivative of the momentum map and the tangent space to the group orbit at a $\mathbf{C}_{nv}(k_1R, k_2R', k_pp)$ configuration. These expressions are given in the next two propositions. Since $\mathbf{C}_{nv}$ refers to fixed vertical reflexion planes, the values of ϕ^0_j in (3.1) above can be taken to be:

$$\phi^0_j = \begin{cases} 0 & \text{if } j = 1 \dots k_1 \\ \pi/n & \text{if } j = (k_1+1) \dots k_r \end{cases}$$

where $k_r = k_1 + k_2$ is the total number of rings.

Proposition 3.1. *At a $\mathbf{C}_{nv}(k_1R, k_2R', k_pp)$ configuration, the differential of the momentum map is as follows: let*

$$\mathbf{u} = \sum_{j,\ell} \left(a^{(\ell)}_{j,\theta}\alpha^{(\ell)}_{j,\theta} + a^{(\ell)}_{j,\phi}\alpha^{(\ell)}_{j,\phi} + b^{(\ell)}_{j,\theta}\beta^{(\ell)}_{j,\theta} + b^{(\ell)}_{j,\phi}\beta^{(\ell)}_{j,\phi} \right) + \sum_{j\ polar} (c_j\delta x_j + d_j\delta y_j),$$

be a tangent vector (the $a^{(\ell)}_{j,\theta}$ etc. are its components with respect to the Fourier basis, where j numbers the rings and ℓ the modes in each ring), then

$$\begin{aligned} &\mathsf{d}\Phi(\mathbf{u}) \\ = \quad & \sum_{j=1}^{k_r} \kappa_j \cos\theta_j (a^{(1)}_{j,\theta} + \mathsf{i}b^{(1)}_{j,\theta}) + \mathsf{i}\sum_{j=1}^{k_r} \kappa_j \sin\theta_j (a^{(1)}_{j,\phi} + \mathsf{i}b^{(1)}_{j,\phi}) + \sum_{j\ polar} \kappa_j (c_j + \mathsf{i}d_j) \\ & \bigoplus - \sum_{j=1}^{k_r} \kappa_j \sin\theta_j a^{(0)}_{j,\theta} \end{aligned}$$

where the direct sum corresponds to the $\mathbf{C}_{nv}$-invariant decomposition of $\mathfrak{so}(3)^*$ as a direct sum of a plane (the 'x-y-plane') and the line $\mathrm{Fix}(\mathbf{C}_{nv}, \mathfrak{so}(3)^*)$ *(the 'z-axis').*

This is proved from the definition of the momentum map (2.2), and some Fourier type calculations. The kernel of the momentum map is readily read off from this. The following proposition results from similar calculations involving the infinitesimal rotation matrices in $\mathbb{R}^3$:

Proposition 3.2. *Let x_e be a $\mathbf{C}_{nv}(k_1R, k_2R', k_pp)$ configuration, and $\mu = \Phi(x_e)$. If $\mu \neq 0$, then the tangent space to the orbit $\mathfrak{so}(3)_\mu \cdot x_e$ is generated by the vector*

$$\sum_{j=1}^{k_r} \alpha^{(0)}_{j,\phi}.$$

If $\mu = 0$, then $\mathfrak{so}(3)_\mu \cdot x_e = \mathfrak{so}(3) \cdot x_e$ and is generated by the vector above, and the following two other vectors,

$$\sum_{j=1}^{k_r} \left(\beta_{j,\theta}^{(1)} + \cot\theta_j\, \alpha_{j,\phi}^{(1)}\right) + \sum_{j\ polar} \operatorname{sign}(z_j)\, \delta y_j,$$

$$\sum_{j=1}^{k_r} \left(\alpha_{j,\theta}^{(1)} - \cot\theta_j\, \beta_{j,\phi}^{(1)}\right) + \sum_{j\ polar} \operatorname{sign}(z_j)\, \delta x_j.$$

Now, $\mathfrak{so}(3)_\mu \cdot x_e \subset \ker \mathsf{d}\Phi_{x_e}$ and the symplectic slice $\mathcal{N}$ is the orthogonal complement to the former inside $\ker \mathsf{d}\Phi$ (or indeed any complementary subspace, not necessarily orthogonal, though to take advantage of the symmetry group the subspace should chosen to be invariant under G_{x_e}).

3.2. **Single ring.** Let x_e be a $\mathbf{C}_{nv}(R, k_p p)$ configuration, a single ring of n vortices together with k_p polar vortices where, of course, $k_p = 0, 1$ or 2. Since there is only one ring, we write $\alpha_\theta^{(\ell)}, \beta_\theta^{(\ell)}$ etc. instead of $\alpha_{1,\theta}^{(\ell)}, \beta_{1,\theta}^{(\ell)}$ etc.

Proposition 3.3. *For these single ring configurations, the symplectic slice can be decomposed by Fourier modes (or isotypic representations) as*

$$\mathcal{N} = \bigoplus_{\ell=1}^{[n/2]} V_\ell,$$

where for $\ell \geq 2$,

$$V_\ell = \left\langle \alpha_\theta^{(\ell)}, \alpha_\phi^{(\ell)}, \beta_\theta^{(\ell)}, \beta_\phi^{(\ell)} \right\rangle$$

(with the understanding that $\beta_\theta^{(n/2)} = \beta_\phi^{(n/2)} = 0$ when n is even). So $\dim V_\ell = 4$ for $1 < \ell < n/2$, and if n is even $\dim V_{n/2} = 2$. Furthermore,

$$\dim V_1 = \begin{cases} 2k_p + 2 & \text{if } \mu \neq 0 \text{ and } n > 2 \\ 2k_p & \text{if } \mu = 0 \text{ and } n > 2 \\ 2k_p & \text{if } \mu \neq 0 \text{ and } n = 2 \\ \max\{0, 2k_p - 2\} & \text{if } \mu = 0 \text{ and } n = 2. \end{cases}$$

A basis for V_1 follows from Propositions 3.1 and 3.2, and is given in the relevant section.

Representations As representations of $G_{x_e} \simeq \mathbf{C}_{nv} \simeq \mathbf{D}_n$ and $G_{x_e}^0 \simeq \mathbf{C}_n$, the V_ℓ are pairwise distinct, so by Schur's Lemma both the Hessian $\mathsf{d}^2 H_\xi|_{\mathcal{N}}$ and the linearized vector field $L_{\mathcal{N}}$ block diagonalize with respect to this decomposition. We now give a brief description of these representations. These statements follow directly from the definition of the Fourier modes in (3.1) above.

For $2 < \ell < n/2$, the Fourier subspace V_ℓ is 4-dimensional, and consists of a direct sum of two 2-dimensional symplectic irreducibles, one isomorphic to the usual representation of $\mathbf{C}_n$ acting on the plane with 'speed' ℓ (that is, a rotation by ρ in $\mathbf{C}_n$ acts on the plane by a rotation through $\ell\rho$), and the other the dual representation. Of course, the reflexions in $\mathbf{C}_{nv}$ act antisymplectically.

For $\ell = n/2$ (when n is even), $V_{n/2}$ is 2-dimensional, with $G_{x_e}^0$ acting by $\{\pm I\}$, but G_{x_e} acting by reflexion in a line. More specifically, $V_{n/2} = \left\langle \alpha_\theta^{(n/2)}, \alpha_\phi^{(n/2)} \right\rangle$ and

one generator of G_{x_e} acts trivially on $\alpha_\theta^{(n/2)}$ and by -1 on $\alpha_\phi^{(n/2)}$, while another acts the other way around.

The subspace V_1 is more involved. The representations $\left\langle \alpha_\theta^{(1)}, \beta_\theta^{(1)} \right\rangle$, $\left\langle \alpha_\phi^{(1)}, \beta_\phi^{(1)} \right\rangle$ and $\langle \delta x_j, \delta y_j \rangle$ $(j = 1, \ldots, k_p)$ do not lie in the symplectic slice, and it is necessary to use Propositions 3.1 and 3.2 to write down the bases of V_1 which will be central in later calculations. However, the underlying representations are all isomorphic (i.e., ignoring the symplectic structure); they are copies of the basic 2-dimensional representations of the dihedral group $\mathbf{C}_{nv}$, and it follows that V_1 is a direct sum of such representations. But as *symplectic* representations this is more subtle: the subspaces $\langle \delta x_j, \delta y_j \rangle$ are symplectic, while the others mentioned are isotropic.

3.3. **General case.** In the general case where x_e is a $\mathbf{C}_{nv}(k_1R, k_2R', k_pp)$ configuration ($k_p = 0, 1$ or 2), we have the following decomposition.

Proposition 3.4. *For these multiring configurations, the symplectic slice decomposes as a direct sum of Fourier modes*

$$\mathcal{N} = \bigoplus_{\ell=0}^{[n/2]} V_\ell$$

where for $2 \leq \ell \leq [n/2]$,

$$V_\ell = \left\langle \alpha_{j,\theta}^{(\ell)}, \alpha_{j,\phi}^{(\ell)}, \beta_{j,\theta}^{(\ell)}, \beta_{j,\phi}^{(\ell)} \mid j = 1 \ldots k_r \right\rangle,$$

which is of dimension $4k_r$ *if* $\ell < n/2$ *and* $2k_r$ *if* $\ell = n/2$, *where* k_r *is the total number of rings. The subspaces* V_0 *and* V_1 *are subspaces of the corresponding spaces determined by Propositions 3.1 and 3.2 and are given in the relevant sections.*

The spaces V_ℓ as representations of G_{x_e} and $G_{x_e}^0$ and $2 \leq \ell \leq n/2$ will just be the sum of several copies of the corresponding V_ℓ for a single ring.

4. **Bifurcations and symmetry.** The configurations we consider in this paper depend on a number of parameters, both external and internal (the internal parameter is the conserved momentum, the external ones the vorticity). As a result, one finds many bifurcations and since the system has symmetry, the bifurcations will reflect this symmetry, and in particular will depend on how the symmetry group of a given relative equilibrium (RE) acts on the eigenspace in which the bifurcation occurs. Of course, the transitions involving a change in stability are such bifurcations. Here we present a brief zoology of the bifurcations that are encountered.

The simplest steady-state bifurcation in a Hamiltonian system is the saddle-node, where two equilibria come together and vanish. However, because we are considering symmetric relative equilibria (RE), there is always a 'central' symmetric RE which persists throughout the bifurcation and so the saddle-node will not arise. Consequently, the simplest bifurcation we encounter is the pitchfork.

Some details about how the action of the symmetry group influence which steady-state bifurcations to expect generically were elaborated in [9], see also [4] for a summary. However, only symplectic actions were considered there (without time-reversing symmetries), and the extra time-reversing symmetries restrict what happens generically so their results are not directly applicable.

Remark 4.1. When the relative equilibrium (or reduced equilibrium) has a mode with imaginary eigenvalues, one can apply the symmetry methods of [29, 30] to find

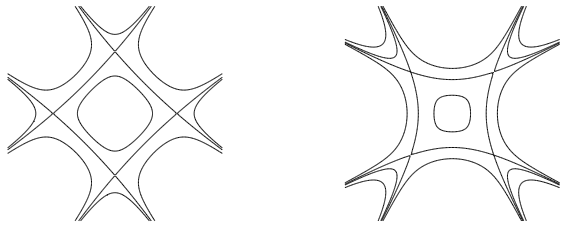

(a) Transcritical $\mathbf{D}_4$-pitchfork

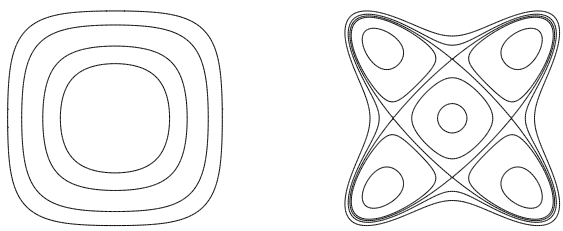

(b) 'Standard' $\mathbf{D}_4$-pitchfork

FIGURE 4.1. Contours of the generic 1-parameter family of $\mathbf{D}_4$-invariant functions in the plane $H_\lambda(z) = \lambda|z|^2 + a|z|^4 + b\,\mathrm{Re}(z^4) + O(z^5)$. The top pair (a) represent a transcritical bifurcation and occur if $|a| < |b|$, while the bottom pair (c) and (d) represent a standard pitchfork bifurcation, occurring if $|a| > |b|$. In both cases the left-hand figure represents $\lambda < 0$ and the right-hand one $\lambda > 0$. (Distinguishing between sub- and super-critical cases depends on stability information in other 'modes'.) See text for how these relate to other dihedral groups.

families of relative periodic orbits in a neighbourhood of the relative equilibrium with prescribed spatio-temporal symmetries. We do not pursue this here.

4.1. **Symmetric pitchfork bifurcations.** In this bifurcation, there is a central 'core' RE which persists throughout the bifurcation, and whose eigenvalues (of the linearization) pass through zero as parameters are varied. As the transition occurs, other RE branch off from the central one. In our setting this bifurcation occurs with the symmetry of a dihedral group $\mathbf{D}_k$ (where k depends on both ℓ and n).

One can distinguish between transcritical pitchfork bifurcations on the one hand and standard pitchforks on the other; in the former there are bifurcating solutions on both sides of the bifurcation point, while in the latter the bifurcating solutions all coexist for the same parameter values: see Figure 4.1. Which occurs depends principally on the value of k. A typical pitchfork bifurcation with $\mathbf{D}_3$ symmetry is transcritical, analogous to (a) in the figure but with 3-fold symmetry, while a typical pitchfork with $\mathbf{D}_k$-symmetry for $k > 4$ is a standard pitchfork analogous to (b) but again with k-fold symmetry. If $k = 4$ then either case can occur, as described in the figure.

Note that if a standard pitchfork bifurcation involves a change in stability then it is either sub- or super-critical, depending on whether the bifurcating solutions are stable or unstable respectively.

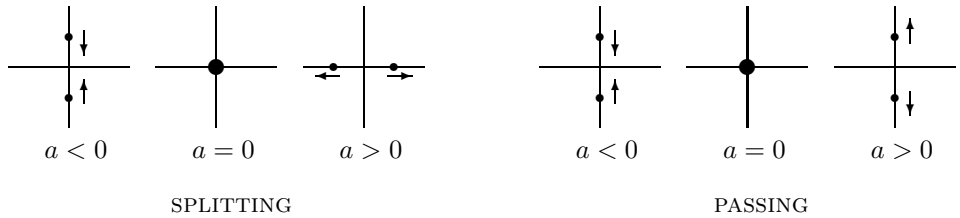

FIGURE 4.2. The two scenarios for the generic movement of eigenvalues in symmetric steady-state pitchfork bifurcation.

In the bifurcations occurring in this paper, if the symmetry is $\mathbf{C}_{nv} \simeq \mathbf{D}_n$, and the bifurcation is in mode ℓ, then the effective symmetry for the bifurcation is $\mathbf{D}_k$ where $k = n/(n,\ell)$, where (n,ℓ) is the highest common factor of n and ℓ. This is because all points in this mode have $\mathbb{Z}_{(n,\ell)}$-symmetry, see (3.3), leaving an effective action of $\mathbf{D}_n/\mathbb{Z}_{(n.\ell)} \simeq \mathbf{D}_k$.

For example, if n is even and $\ell = n/2$ then $k = 2$ and there is an effective action of $\mathbf{D}_2 \simeq \mathbb{Z}_2 \times \mathbb{Z}_2$, and all points of this mode have $\mathbb{Z}_{n/2}$-symmetry. It follows that if the bifurcation involves this mode, then all bifurcating solutions have at least this symmetry. In fact an analysis of the generic bifurcation shows that they have a further $\mathbb{Z}_2$ giving $\mathbf{D}_{n/2}$ symmetry. The generic pitchfork bifurcation in this mode is the well-known one where there are two branches of bifurcating solutions and a $\mathbb{Z}_2$-symmetry is lost; since the central equilibrium has $\mathbf{D}_n$ symmetry the bifurcating solutions will still have a $\mathbf{D}_{n/2}$-symmetry.

At the other extreme, if n and ℓ are coprime, then $k = n$ and the bifurcating solutions have only $\mathbb{Z}_2$-symmetry, generated by one of the reflexions in $\mathbf{D}_n$.

Figures 5.1 and 5.2 show symmetries of bifurcating solutions.

As the eigenvalues pass through zero in either type of pitchfork bifurcation there are two possibilities, the so-called *splitting* and *passing* behaviours (see Figure 4.2):

Pitchfork of splitting type: This is the familiar scenario where a complex conjugate pair of imaginary eigenvalues of the linear system collide at 0 and then become real and opposite. The central (relative) equilibrium is then possibly elliptic or Lyapounov stable on one side of the bifurcation, and linearly unstable on the other.

Pitchfork of passing type: This is similar, except that the eigenvalues pass through each other and remain on the imaginary axis. See Figure 4.2. If the central RE is say Lyapounov stable (or elliptic) before the bifurcation, then in a pitchfork of passing type the central RE becomes (remains) elliptic, and in the standard pitchfork bifurcation k of the bifurcating solutions are Lyapounov stable (elliptic) while the other k are linearly unstable. In the transcritical case, all the bifurcating RE are linearly unstable.

For example, if a bifurcation takes place due to a degeneracy in the mode space $V_{n/2}$, then generically it will be a standard $\mathbb{Z}_2$-pitchfork bifurcation, and the central relative equilibrium will pass from being (Lyapounov) stable to being linearly unstable. A study of higher order terms will distinguish between standard sub- and super-critical pitchfork bifurcations (something we don't do in this paper).

If on the other hand a bifurcation occurs in the mode V_ℓ with $0 < \ell < n/2$ then generically one may see pitchforks of either passing or splitting type.

4.2. **Hamiltonian Hopf bifurcation.** This occurs when two imaginary eigenvalues of a (relative) equilibrium collide and move off the imaginary axis. This can only happen if the (reduced) Hessian matrix at the (relative) equilibrium is not definite.

There are two possible scenarios depending on the higher order terms:
(a) the two Lyapounov modes associated with the two imaginary eigenvalues are globally connected, and the set of all of these collapse to a point as the eigenvalues collide, and
(b) the two Lyapounov modes are not part of the same family, and as the eigenvalues move off the imaginary axis, so the two families connect and move away from the (relative) equilibrium.

For a detailed description of the bifurcations of periodic and relative periodic orbits that can be expected in this case see [23, 21, 7, 4].

4.3. **Bifurcations from zero momentum.** Consider a relative equilibrium x_0 in a system with $\mathsf{SO}(3)$-symmetry with zero momentum, whose reduced Hessian is non-degenerate.

If the angular velocity of the RE is non-zero, then through that RE there is a curve of RE parametrized by μ. If the reduced Hessian of x_0 is positive definite (so x_e is Lyapounov stable) then generically on one side of the curve the RE is also Lyapounov stable, while on the other it is elliptic, [26].

The genericity assumption is that the frequency of the rotation of the RE (which is $|\xi|$) is distinct from the frequencies of the normal modes of the reduced system. This *ro-vibrational resonance* is discussed briefly at the end of [25], where it is made clear how it is related to the Hamiltonian Hopf bifurcation; the associated dynamics is the subject of a paper by Patrick [37], where he calls it group-reduced resonance. This resonance phenomenon can be seen for a ring and 2 polar vortices in Section 9. The bifurcations arising as parameters are varied have not been studied.

If on the other hand the angular velocity of x_0 is zero then for each non-zero μ there are at least 6 RE, and if x_0 is definite as above, then at least 2 of these are each of Lyapounov stable, elliptic and unstable. Moreover, if the equilibrium in question has symmetry, then the symmetry can be used to give precise estimates for the numbers of RE in a neighbourhood. Details can be found in [28] and a study of deformations from zero velocity to non-zero velocity can be found in [26].

5. **A ring of identical vortices: $\mathbf{C}_{nv}(R)$.** The linear stability of $\mathbf{C}_{nv}(R)$ relative equilibria was determined by Polvani and Dritschel in [38]. A few years ago, Boatto and Cabral [3] studied their Lyapounov stability and found that the two types of stability coincide: whenever the relative equilibrium fails to be Lyapounov stable the linearization of X_H has real eigenvalues. In this section, we give another proof using the geometric method of this paper. The calculations are also used in later sections.

5.1. **Symplectic slice.** For n vortices of unit vorticity the Hamiltonian is

$$H(\theta_j, \phi_j) \;=\; -\sum_{j<k} \ln\left(1 - \sin\theta_j \sin\theta_k \cos(\phi_j - \phi_k) - \cos\theta_j \cos\theta_k\right) \tag{5.1}$$

and the augmented Hamiltonian is $H_\xi = H - \xi \sum_j \cos\theta_j$.

Let x_e be a $\mathbf{C}_{nv}(R)$ relative equilibrium and θ_0 the co-latitude of the ring. The angular velocity of x_e is

$$\xi \;=\; \frac{(n-1)\cos\theta_0}{\sin^2\theta_0},$$

since H_ξ has a critical point there and $\frac{\partial H_\xi}{\partial \theta_j}(x_e) = \frac{(n-1)\cos\theta_0 - \xi\sin^2\theta_0}{\sin\theta_0}$. The momentum of the relative equilibrium is just $\mu = n\cos\theta_0$.

The second derivatives of H at the relative equilibrium are:

$$\begin{array}{rclrcl}
\frac{\partial^2 H}{\partial\theta_j^2} & = & -\frac{(n-1)(n-5)}{6\sin^2\theta_0} & \frac{\partial^2 H}{\partial\theta_j\partial\theta_k} & = & \frac{1}{2\sin^2\theta_0\sin^2(\pi(j-k)/n)} \\
\frac{\partial^2 H}{\partial\theta_j\partial\phi_j} & = & 0 & \frac{\partial^2 H}{\partial\theta_j\partial\phi_k} & = & 0 \\
\frac{\partial^2 H}{\partial\phi_j^2} & = & \frac{1}{6}(n^2-1) & \frac{\partial^2 H}{\partial\phi_j\partial\phi_k} & = & -\frac{1}{2\sin^2(\pi(j-k)/n)}.
\end{array}$$

We note that $\sum_{r=1}^{n-1} 1/\sin^2(\pi r/n) = \frac{1}{3}(n^2-1)$ [11].

Notation In order to harmonize the statements of the results between n even and n odd, we introduce the following notation: let $\eta_1^{(\ell)}, \eta_2^{(\ell)}, \eta_3^{(\ell)}, \eta_4^{(\ell)}$ be objects defined for all $2 \le \ell \le \left[\frac{n-1}{2}\right]$, where $[m]$ is the integer part of $m \in \mathbb{N}$, and only $\eta_1^{(\ell)}, \eta_2^{(\ell)}$ for $\ell = n/2$ when n is even. Then define

$$\left\{\eta_1^{(\ell)}, \eta_2^{(\ell)}, \eta_3^{(\ell)}, \eta_4^{(\ell)} \mid 2 \le \ell \le [n/2]\right\}^*$$

to be

$$\left\{\begin{array}{lcl}
\text{for even } n & : & \left\{\eta_1^{(\ell)}, \eta_2^{(\ell)}, \eta_3^{(\ell)}, \eta_4^{(\ell)} \mid 2 \le \ell \le \frac{n}{2}-1\right\} \cup \left\{\eta_1^{(n/2)}, \eta_2^{(n/2)}\right\} \\
\text{for odd } n & : & \{\eta_1^{(\ell)}, \eta_2^{(\ell)}, \eta_3^{(\ell)}, \eta_4^{(\ell)} \mid 2 \le \ell \le [n/2]\}.
\end{array}\right. \tag{5.2}$$

In Proposition 3.3 a basis is given for each of the V_ℓ except for $\ell = 1$. The following proposition does the same for V_1.

Proposition 5.1. *For $n = 2$ the symplectic slice is 0. For $n \ge 3$, the symplectic slice decomposes as $\mathcal{N} = \bigoplus_{\ell=1}^{[n/2]} V_\ell$, where for $\mu \ne 0$*

$$\dim V_\ell = \begin{cases} 2 & \text{if } \ell = 1 \text{ or } n/2 \\ 4 & \text{otherwise.} \end{cases}$$

If $\mu = 0$ then $V_1 = 0$, while for $\mu \ne 0$, $V_1 = \langle e_1, e_2\rangle$, where

$$\begin{array}{rcl} e_1 & = & \sin\theta_0\ \alpha_\theta^{(1)} + \cos\theta_0\ \beta_\phi^{(1)} \\ e_2 & = & \sin\theta_0\ \beta_\theta^{(1)} - \cos\theta_0\ \alpha_\phi^{(1)}. \end{array}$$

With respect to the resulting basis for the symplectic slice, the Hessian $\mathsf{d}^2 H_\xi|_{\mathcal{N}}(x_e)$ is diagonal, and $L_{\mathcal{N}}$ block diagonalizes in 2×2 blocks.

Proof. It is straightforward to check that the vectors above do form a basis for V_1 at x_e thanks to Propositions 3.1 and 3.2.

The Hessian $\mathsf{d}^2 H_\xi|_{\mathcal{N}}(x_e)$ and the linearization $L_{\mathcal{N}}$ are both $G^0_{x_e}$-invariant. Assume n odd. It follows from Section 3.2 and Schur's Lemma (see the introduction) that $\mathsf{d}^2 H_\xi|_{\mathcal{N}}(x_e)$ and $L_{\mathcal{N}}$ both block diagonalize into 4×4 blocks and one 2×2 block corresponding to the subspaces

$$V_\ell = \left\langle \alpha_\theta^{(\ell)}, \beta_\theta^{(\ell)}, \alpha_\phi^{(\ell)}, \beta_\phi^{(\ell)} \right\rangle$$

and $\langle e_1, e_2\rangle$, respectively. See the proof of Theorem 4.5 of [15] for a detailed proof of a similar assertion.

Now fix ℓ and denote by s an anti-symplectic (time-reversing) element of G_{x_e}. For example s could be the reflexion $y \mapsto -y$ together with an order two permutation of S_n. The restriction of H_ξ to V_ℓ is $\mathbb{Z}_2[s]$-invariant. Moreover $\left\langle \alpha_\theta^{(\ell)}, \beta_\phi^{(\ell)} \right\rangle$ and $\left\langle \beta_\theta^{(\ell)}, \alpha_\phi^{(\ell)} \right\rangle$ are non-isomorphic irreducible representation of $\mathbb{Z}_2[s]$ on V_ℓ. Hence $\mathsf{d}^2 H_\xi|_{\mathcal{N}}(x_e)$ block diagonalizes into 2×2 blocks which correspond to subspaces $\left\langle \alpha_\theta^{(\ell)}, \beta_\phi^{(\ell)} \right\rangle$, $\left\langle \beta_\theta^{(\ell)}, \alpha_\phi^{(\ell)} \right\rangle$, and $\langle e_1, e_2\rangle$. This result does not depend on the details of the Hamiltonian, only its symmetries. However taking account of its particular form, one can improve the block diagonalization. Indeed one has

$$\mathsf{d}^2 H_\xi(x_e)\cdot(\alpha_\theta^{(\ell)}, \beta_\phi^{(\ell)}) \;=\; \mathsf{d}^2 H_\xi(x_e)\cdot(\beta_\theta^{(\ell)}, \alpha_\phi^{(\ell)}) \;=\; 0$$

and $\mathsf{d}^2 H_\xi(x_e)\cdot(e_1, e_2) = 0$ which gives the desired diagonalization of the Hessian.

The particular form of the symplectic form also enables us to improve the diagonalization of $L_{\mathcal{N}}$. Among the basis vectors of V_ℓ, only $\omega(\alpha_\theta^{(\ell)}, \alpha_\phi^{(\ell)})$ and $\omega(\beta_\theta^{(\ell)}, \beta_\phi^{(\ell)})$ do not vanish, and so the restriction of ω to V_ℓ block diagonalizes into two 2×2 blocks which correspond to the subspaces $\left\langle \alpha_\theta^{(\ell)}, \alpha_\phi^{(\ell)} \right\rangle$ and $\left\langle \beta_\theta^{(\ell)}, \beta_\phi^{(\ell)} \right\rangle$. The block diagonalization of $L_{\mathcal{N}}$ then follows from $L_{\mathcal{N}} = \mathbf{J}_{\mathcal{N}} \mathsf{d}^2 H_\xi|_{\mathcal{N}}(x_e)$.

The case n even is very similar, except that there is an additional 2×2 block in the $G^0_{x_e}$-isotypic decomposition, and leads to the same result. □

5.2. **Stability.** The block diagonalization of $\mathsf{d}^2 H_\xi|_{\mathcal{N}}(x_e)$ and $L_{\mathcal{N}}$ enable us to find formulae for their eigenvalues, and thus to conclude criteria for both Lyapounov and linear stability.

Theorem 5.2. *The stability of a ring of n identical vortices depends on n and the co-latitude θ_0 as follows:*

n	*condition for stability*
2, 3	*all* θ_0
4	$\cos^2\theta_0 > 1/3$
5	$\cos^2\theta_0 > 1/2$
6	$\cos^2\theta_0 > 4/5$
≥ 7	*always linearly unstable*

For $n = 4, 5, 6$, the ring is linearly unstable if the inequality is reversed.

Proof. Any arrangement of two vortices is a relative equilibrium [12]. When perturbing such a relative equilibrium, we obtain a new relative equilibrium close to the first. Thus any relative equilibrium of two vortices is Lyapounov stable modulo $\mathsf{SO}(2)$ (and modulo $\mathsf{SO}(3)$ if $\mu = 0$).

Now assume $n \geq 3$. We first study Lyapounov stability. Suppose further that $\mu \neq 0$ and so the ring is not equatorial. A simple calculation shows that $\mathsf{d}^2 H_\xi(x_e)\cdot(\beta_\theta^{(\ell)}, \beta_\theta^{(\ell)}) = \mathsf{d}^2 H_\xi(x_e)\cdot(\alpha_\theta^{(\ell)}, \alpha_\theta^{(\ell)})$ and $\mathsf{d}^2 H_\xi(x_e)\cdot(\beta_\phi^{(\ell)}, \beta_\phi^{(\ell)}) = \mathsf{d}^2 H_\xi(x_e)\cdot(\alpha_\phi^{(\ell)}, \alpha_\phi^{(\ell)})$. Hence it follows from Proposition 5.1 that

$$\mathsf{d}^2 H_\xi|_{\mathcal{N}}(x_e) \;=\; \operatorname{diag}\left(\lambda_1, \lambda_1, \{\lambda_\theta^{(\ell)}, \lambda_\phi^{(\ell)}, \lambda_\theta^{(\ell)}, \lambda_\phi^{(\ell)} \mid 2 \leq \ell \leq [n/2]\}^*\right)$$

(recall notation from (5.2)) where

$$\begin{aligned}\lambda_1 &= \sin^2\theta_0\lambda_\theta^{(1)} + \cos^2\theta_0\lambda_\phi^{(1)},\\ \lambda_\theta^{(\ell)} &= \mathsf{d}^2H_\xi(x_e)\cdot(\alpha_\theta^{(\ell)},\alpha_\theta^{(\ell)}),\\ \lambda_\phi^{(\ell)} &= \mathsf{d}^2H_\xi(x_e)\cdot(\alpha_\phi^{(\ell)},\alpha_\phi^{(\ell)}).\end{aligned}$$

Thanks to the following formula [11, p.271]

$$\sum_{j=1}^{n-1}\frac{\cos(2\pi\ell j/n)}{\sin^2(\pi j/n)} = \frac{1}{3}(n^2-1)-2\ell(n-\ell),$$

we find after some computations that $\lambda_\phi^{(\ell)} = n\ell(n-\ell)/2$ and

$$\lambda_\theta^{(\ell)} = \frac{n}{2\sin^2\theta_0}\left[-(\ell-1)(n-\ell-1)+(n-1)\cos^2\theta_0\right]. \tag{5.3}$$

The eigenvalues $\lambda_\phi^{(\ell)}$ are all positive and $\lambda_1 = n(n-1)\cos^2\theta_0 > 0$. The relative equilibrium is therefore Lyapounov stable (modulo $\mathsf{SO}(2)$) if $(n-1)\cos^2\theta_0 > (\ell-1)(n-\ell-1)$ for all $\ell = 2,\dots,[n/2]$, that is if $\cos^2\theta_0 > ([n/2]-1)(n-[n/2]-1)/(n-1) = \frac{1}{n-1}\left[\frac{n^2}{4}\right]-1$. This gives the desired values.

We now turn to linear stability. It follows from Proposition 5.1 and the block diagonalization of $\mathsf{d}^2H_\xi|_{\mathcal{N}}(x_e)$ that

$$L_{\mathcal{N}} = \operatorname{diag}\left(\begin{pmatrix}0 & -\lambda_1\\ \lambda_1 & 0\end{pmatrix}, \left\{\begin{pmatrix}0 & -\lambda_\phi^{(\ell)}\\ \lambda_\theta^{(\ell)} & 0\end{pmatrix}, \begin{pmatrix}0 & -\lambda_\phi^{(\ell)}\\ \lambda_\theta^{(\ell)} & 0\end{pmatrix} \mid 2\le\ell\le[n/2]\right\}^*\right)$$

where the blocks are given up to a strictly positive scalar factor. The eigenvalues of $L_{\mathcal{N}}$ are therefore

$$\pm\mathrm{i}\lambda_1, \left\{\pm\mathrm{i}\sqrt{\lambda_\theta^{(\ell)}\lambda_\phi^{(\ell)}} \mid 2\le\ell\le[n/2]\right\},$$

(up to a positive factor) and so the relative equilibrium is linearly unstable if $\lambda_\theta^{(\ell)} < 0$ for some ℓ, that is if

$$\cos^2\theta_0 < \frac{1}{n-1}\left[\frac{n^2}{4}\right]-1.$$

In particular this inequality is satisfied if $\theta_0 = \pi/2$ and $n > 3$.

When the ring is equatorial, one has $\theta_0 = \pi/2$ and $\mu = 0$. In particular $\lambda_1 = 0$. This is because the symplectic slice is smaller ($G_\mu = \mathsf{SO}(3)$ for $\mu = 0$): it follows from Proposition 3.2 that we have to remove the vectors e_1, e_2 from the basis for $\mu \neq 0$ (that is to remove λ_1 from the previous eigenvalue study). However, this does not change the instability results, as the instability is primarily due to the $\ell = [n/2]$ mode. It follows that the $\mathbf{C}_{nv}$ equatorial relative equilibria are linearly unstable for $n > 3$, and Lyapounov stable (modulo $\mathsf{SO}(3)$) for $n = 3$. □

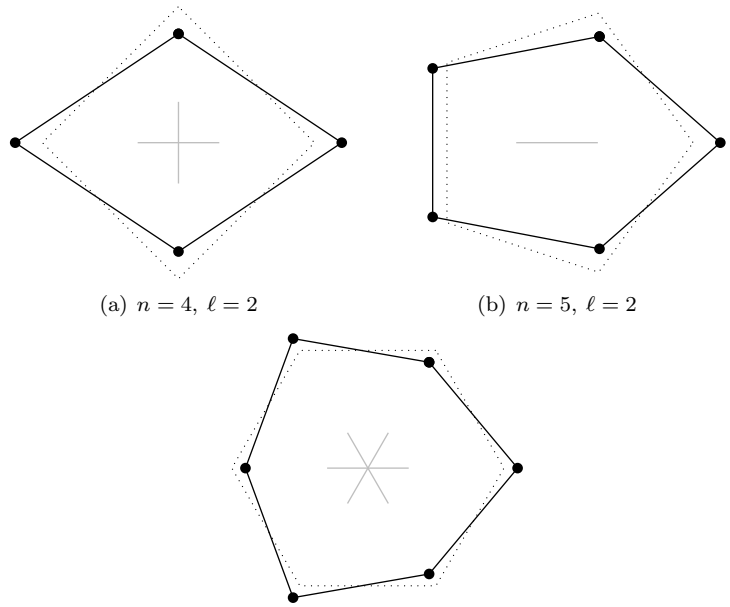

(a) $n = 4,\ \ell = 2$ (b) $n = 5,\ \ell = 2$

(c) $n = 6,\ \ell = 3$

FIGURE 5.1. Polar view of the $\ell = [n/2]$ bifurcations for $n = 4, 5, 6$. The dotted lines represent the 'central' relative equilibrium with $\mathbf{D}_n = \mathbf{C}_{nv}$ symmetry, while the dots are the vortices of the (stable) bifurcating relative equilibrium with lower symmetry; the grey lines in the centre of each represent the lines of reflexion. The figures would be rotating in time.

5.3. **Bifurcations.** The loss of stability of the ring is as usual accompanied by a bifurcation. The proof above shows that the 'critical mode' for stability is $\ell = [n/2]$. For $n \geq 7$ a ring is always unstable to this mode, while for $4 \leq n \leq 6$ the ring is stable when sufficiently close to the pole, and loses stability to this mode as it moves closer to the equator. Here we describe the bifurcations that accompany this loss of stability.

There is another bifurcation that occurs in all rings with $n \geq 6$, namely in the $\ell = 2$ mode. Indeed, expression (5.3) shows that only the modes $\ell = 2$ and $\ell = [n/2]$ can satisfy $\lambda_\theta^{(\ell)} = 0$ (the former at $\cos^2\theta_0 = \frac{n-3}{n-1}$). We are only considering 'relative steady-state' bifurcations, so where the eigenvalues pass through zero.

The dihedral symmetry in each mode dictates the type of bifurcation to expect: if $\ell = n/2$ so $\dim V_\ell = 2$, one has a $\mathbb{Z}_2$-pitchfork bifurcation involving a loss of $\mathbb{Z}_2$-symmetry. On the other hand if $\dim V_\ell = 4$ then there is a pitchfork bifurcation with dihedral symmetry. See Section 4 for a discussion of these. Here we describe briefly the bifurcations arising for low values of n: the pattern continues for larger n.

- **n = 3:** There is no bifurcation: the relative equilibrium is always Lyapounov stable (relative to $\mathsf{SO}(2)$ if $\mu \neq 0$ and to $\mathsf{SO}(3)$ if $\mu = 0$).
- **n = 4:** The only bifurcation occurring is when $\cos^2\theta_0 = 1/3$ where the stability of the ring changes. The mode $\ell = 2$ which is involved in the bifurcation is

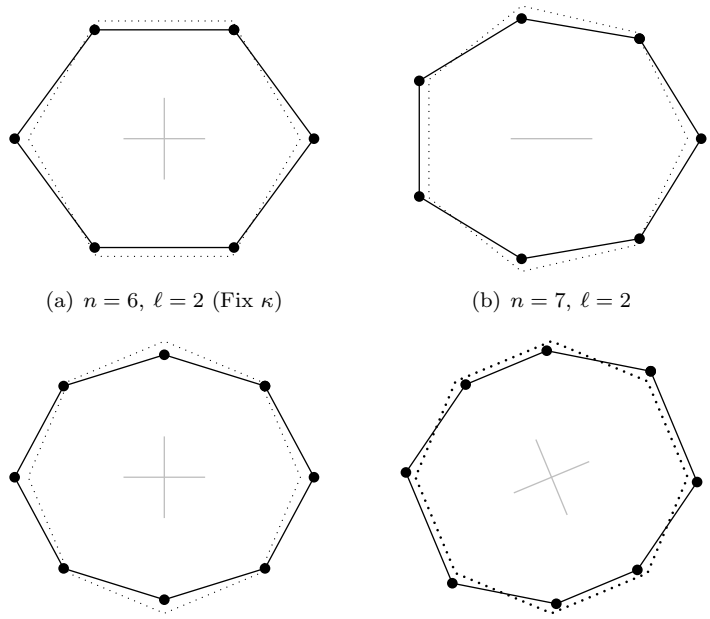

(a) $n = 6$, $\ell = 2$ (Fix κ)

(b) $n = 7$, $\ell = 2$

(c) $n = 8$, $\ell = 2$ (Fix κ)

(d) $n = 8$, $\ell = 2$ (Fix κ')

FIGURE 5.2. Perturbations of the n-ring in the mode $\ell = 2$. These configurations are invariant under a subgroup isomorphic to $\mathbb{Z}_2$ or $\mathbb{Z}_2 \times \mathbb{Z}_2$ according to the parity of n, and the grey lines in the centre of each represent the lines of reflexion. The dotted figures are the regular n-gons.

of dimension 2, spanned by $\alpha_\theta^{(2)}$, $\alpha_\phi^{(2)}$. It is the eigenvalue corresponding to $\alpha_\theta^{(2)}$ that passes through zero, which tells us the symmetry of the bifurcating relative equilibria: they consists of a pair of 2-rings on different latitudes, denoted $\mathbf{C}_{2v}(R, R')$, as shown in Figure 5.1(a).

n = 5: Again the only bifurcation occurs in the $\ell = 2$ mode when $\theta_0 = \pi/4$ and $3\pi/4$. This mode is 4-dimensional, with an action of $\mathbf{D}_5$. For θ close to these values (and either above or below: we have not calculated the higher order terms to determine this) there are 5 saddle points (unstable relative equilibria) and 5 other critical points which will be elliptic (and possibly non-linearly stable, depending whether the bifurcation is sub- or super-critical). See Figure 5.1 (b) for a representation of a typical bifurcating solution.

n = 6: In this case there are two bifurcations as the co-latitude increases. The first occurs at $\cos^2\theta_0 = 4/5$ in the $\ell = 3$ mode where the regular hexagon loses stability. Here there is a usual $\mathbb{Z}_2$-pitchfork bifurcation, resulting in a pair of staggered 3-rings (that is, $C_{3v}(R, R')$), which will be elliptic; see Figure 5.1 (c) for a typical bifurcating configuration. The second bifurcation occurs at $\cos^2\theta_0 = 3/5$ in the $\ell = 2$ mode; the effective action will be of $\mathbf{D}_3$ and so if it is generic one expects a transcritical bifurcation. Figure 5.2 (a) shows a typical bifurcating configuration in this mode. Between the two bifurcation values of θ_0, the reduced system has a pair of (double) imaginary eigenvalues

and a pair of real eigenvalues. Closer to the equator, all the eigenvalues are real.

n = 7: Here there is just one bifurcation (the ring is always unstable due to the mode $\ell = 3$, where the linear system has real eigenvalues). It occurs at $\cos^2\theta_0 = 2/3$ in the 4-dimensional $\ell = 2$ mode. This is a $\mathbf{D}_7$-pitchfork, which is a standard pitchfork, and analogous to that shown (for $n = 4$) in Figure 4.1 (b). Whether the bifurcating solutions exist for $\theta > \theta_0$ or for $\theta < \theta_0$ depends on the higher order terms, and we have not analysed these.

n = 8: Again there is just one bifurcation, occurring at $\cos^2\theta_0 = 5/7$. In this case, since again $\ell = 2$ the effective action on V_2 is one of $\mathbf{D}_4$. Depending on the higher order terms, the bifurcation is either transcritical, as in Figure 4.1 (a), or standard pitchfork as in Figure 4.1 (b). (They are not sub- or super-critical as the central equilibrium is unstable throughout the bifurcation.) One type of bifurcating solution will be as depicted in Figure 4.1 (c) while the other will be as in Figure 4.1 (d).

Similar conclusions can be made for $n \geq 9$, where all $\ell = 2$ bifurcations will be standard pitchfork, rather than transcritical. Further calculations involving the higher order terms in the bifurcations occurring here can be found in [32].

6. **A ring with a polar vortex: $\mathbf{C}_{nv}(R,p)$.** A configuration consisting of a ring of identical vortices placed regularly around a line of latitude, together with a single pole either at the North or South pole is always a relative equilibrium, rotating steadily about the 'vertical' axis. We assume that the polar vortex lies at the North pole and its vorticity is κ, while the remaining n vortices are all identical with vortex strength 1 and lie in a regular ring on a fixed circle of co-latitude θ_0.

This relative equilibrium is of symmetry type $\mathbf{C}_{nv}(R,p)$ and denoted x_e. Its momentum is $\Phi(x_e) = (0,0,\mu)$, where $\mu = \kappa + n\cos\theta_0$.

The Hamiltonian is given by

$$H \;=\; H_r + H_p$$

where H_r is the contribution to the total Hamiltonian from the interactions within the ring (5.1), and

$$\begin{aligned} &H_p(x,y,\theta_i,\phi_i) \\ &= -\kappa \sum_{j=1}^{n} \ln\left(1 - x\sin\theta_j\cos\phi_j - y\sin\theta_j\sin\phi_j - \sqrt{1-x^2-y^2}\cos\theta_j\right), \end{aligned}$$

is the Hamiltonian responsible for the interaction of the polar vortex and the ring.

In this case

$$H_\xi \;=\; H - \xi\left(\sum_j \cos\theta_j + \kappa\sqrt{1-x^2-y^2}\right).$$

The $\mathbf{C}_{nv}(R,p)$ relative equilibrium at $x = y = 0,\ \theta_j = \theta_0,\ \phi_j = 2\pi j/n$ has angular velocity

$$\xi \;=\; \frac{(n-1)\cos\theta_0 + \kappa(1+\cos\theta_0)}{\sin^2\theta_0} = \frac{\mu + (\kappa-1)\cos\theta_0}{\sin^2\theta_0}$$

since $\frac{\partial H_\xi}{\partial\theta_j}(x_e) = -\frac{(n-1)\cos\theta_0 + \kappa(1+\cos\theta_0) - \xi\sin^2\theta_0}{\sin\theta_0}$ must vanish.

The second derivatives at the relative equilibrium of H can be derived from those for H_r given in the previous section, together with (for $n > 2$):

$$\begin{array}{rclrcl} \frac{\partial^2 H_p}{\partial \theta_j^2} & = & \frac{\kappa}{1-\cos\theta_0} & \frac{\partial^2 H_p}{\partial x^2} & = & \frac{n\kappa}{2} = \frac{\partial^2 H_p}{\partial y^2} \\ \frac{\partial^2 H_p}{\partial x \partial \theta_j} & = & -\frac{\kappa\cos(2\pi j/n)}{1-\cos\theta_0} & \frac{\partial^2 H_p}{\partial y \partial \theta_j} & = & -\frac{\kappa\sin(2\pi j/n)}{1-\cos\theta_0} \\ \frac{\partial^2 H_p}{\partial x \partial \phi_j} & = & -\frac{\kappa\sin\theta_0\sin(2\pi j/n)}{1-\cos\theta_0} & \frac{\partial^2 H_p}{\partial y \partial \phi_j} & = & \frac{\kappa\sin\theta_0\cos(2\pi j/n)}{1-\cos\theta_0}, \end{array}$$

while the other second derivatives all vanish. Here we have used that $\sum \cos^2(2\pi j/n) = n/2$ for $n > 2$. For $n = 2$ this sum is 2 and one obtains

$$\frac{\partial^2 H_p}{\partial x^2} = \frac{2\kappa}{1-\cos\theta_0} \qquad \frac{\partial^2 H_p}{\partial y^2} = -\frac{2\kappa\cos\theta_0}{1-\cos\theta_0}.$$

6.1. **Symplectic slice.** The following proposition gives the symmetry adapted basis for $\mathbf{C}_{nv}(R,p)$ relative equilibria.

Proposition 6.1. *With the symplectic slice decomposition described in Proposition 3.3, that is $\mathcal{N} = \bigoplus_{\ell=1}^{[n/2]} V_\ell$, and for $n \geq 3$ and $\mu \neq 0$ a basis for V_1 is $\{e_1, e_2, e_3, e_4\}$, where*

$$\begin{cases} e_1 &= \cos\theta_0\, \beta_\phi^{(1)} + \sin\theta_0\, \alpha_\theta^{(1)} \\ e_2 &= \kappa\, \beta_\phi^{(1)} + \frac{n}{2}\sin\theta_0\, \delta x \\ e_3 &= \cos\theta_0\, \alpha_\phi^{(1)} - \sin\theta_0\, \beta_\theta^{(1)} \\ e_4 &= \kappa\, \alpha_\phi^{(1)} - \frac{n}{2}\sin\theta_0\, \delta y\,. \end{cases}$$

With respect to the resulting basis for $\mathcal{N}$, the Hessian $\mathsf{d}^2 H_\xi|_{\mathcal{N}}(x_e)$ block diagonalizes into two 2×2 blocks (corresponding to $\ell = 1$) and $(2n-6)$ 1×1 blocks, and $L_{\mathcal{N}}$ block diagonalizes into one 4×4 block (for $\ell = 1$) and the remaining are 2×2 blocks.

When $\mu = 0$, V_1 drops dimension by 2, and in particular the vectors $e_1 + \frac{2}{n}e_2$ and $e_3 + \frac{2}{n}e_4$ lie in the tangent space to the group orbit so one can take $V_1 = \langle e_1, e_3\rangle$, and in this basis the Hessian restricted to V_1 is diagonal.

The case where $n = 2$ is discussed below.

For later use we record the symplectic form on the space V_1, the values follow from (3.2):

$$\begin{array}{ll} \omega(e_1,\, e_2) = 0 & \omega(e_3,\, e_4) = 0 \\ \omega(e_1, e_3) = n\cos\theta_0 \sin^2\theta_0 & \omega(e_1, e_4) = \frac{1}{2} n\,\kappa \sin^2\theta_0 \\ \omega(e_2, e_3) = \frac{1}{2} n\,\kappa \sin^2\theta_0 & \omega(e_2, e_4) = -\frac{1}{4} n^2 \kappa \sin^2\theta_0. \end{array} \tag{6.1}$$

It follows that $\langle e_1,\, e_2\rangle$ and $\langle e_3,\, e_4\rangle$ are invariant Lagrangian subspaces (and the representation is the sum of an irreducible and its dual).

Proof. The proof is similar to the proof of Proposition 5.1, and we omit the details. □

Using equations (3.3) one sees that the subspaces $\langle e_1,\, e_3\rangle$ and $\langle e_2,\, e_4\rangle$ are invariant and by (6.1 above) they are symplectic. It follows that V_1 is the direct sum of two representations of *complex dual* type [29] (they are dual as on one the orientations defined by ω and by $\mathbf{C}_n$ coincide, while for the other they are opposite).

6.2. **Stability.** The block diagonalizations of the proposition enable us to prove the following stability theorem for $n \geq 4$, illustrated by Figure 6.1. The cases $n = 2$ and 3 are treated afterwards (and illustrated in Figure 6.2).

Theorem 6.2. *A $\mathbf{C}_{nv}(R,p)$ relative equilibrium with $n \geq 4$ and $\mu \neq 0$ is*
(i) Lyapounov stable if

$$\kappa > \kappa_0 \quad \textit{and} \quad \kappa(\kappa + n\cos\theta_0)(a\kappa - b) < 0,$$

(ii) spectrally unstable if and only if

$$\kappa < \kappa_0 \quad \textit{or} \quad 8a\kappa > (n\sin^2\theta_0 + 4(n-1)\cos\theta_0)^2,$$

where

$$\begin{aligned} a &= (1+\cos\theta_0)^2(n\cos\theta_0 - n + 2) \\ b &= (n-1)\cos\theta_0\,(n\sin^2\theta_0 + 2(n-1)\cos\theta_0) \\ \kappa_0 &= \left(\left[\tfrac{(n-2)^2}{4}\right] - (n-1)\cos^2\theta_0\right)/(1+\cos\theta_0)^2. \end{aligned} \tag{6.2}$$

As will be seen in the proof, the conditions involving κ_0 arise from the $\ell = [n/2]$ mode, while the others arise from the $\ell = 1$ mode.

Proof. (i) We first study the Lyapounov stability. Following the beginning of the proof of Theorem 5.2, we obtain from Proposition 6.1 that

$$\mathsf{d}^2 H_\xi|_{\mathcal{N}}(x_e) = \mathrm{diag}(A, A, D)$$

where $D = \mathrm{diag}(\{\lambda_\theta^{(\ell)}, \lambda_\phi^{(\ell)}, \lambda_\theta^{(\ell)}, \lambda_\phi^{(\ell)} \mid 2 \leq \ell \leq [n/2]\}^*)$,

$$A = \begin{pmatrix} q_{11} & q_{12} \\ q_{12} & q_{22} \end{pmatrix}$$

and

$$\begin{aligned} \lambda_\theta^{(\ell)} &= \mathsf{d}^2 H_\xi(x_e)\cdot(\alpha_\theta^{(\ell)}, \alpha_\theta^{(\ell)}) \\ \lambda_\phi^{(\ell)} &= \mathsf{d}^2 H_\xi(x_e)\cdot(\alpha_\phi^{(\ell)}, \alpha_\phi^{(\ell)}) \\ q_{11} &= \mathsf{d}^2 H_\xi(x_e)\cdot(e_1, e_1) \\ q_{12} &= \mathsf{d}^2 H_\xi(x_e)\cdot(e_1, e_2) \\ q_{22} &= \mathsf{d}^2 H_\xi(x_e)\cdot(e_2, e_2). \end{aligned}$$

Note that D exists only for $n \geq 4$. From the previous section one has $\lambda_\phi^{(\ell)} = n\ell(n-\ell)/2$ and some additional computations give

$$\lambda_\theta^{(\ell)} = \frac{n}{2\sin^2\theta_0}\left[-(\ell-1)(n-\ell-1) + (n-1)\cos^2\theta_0 + \kappa(1+\cos\theta_0)^2\right].$$

The eigenvalues $\lambda_\phi^{(\ell)}$ are all positive, thus D is definite if and only if, for all $\ell = 2, \ldots, [n/2]$,

$$\kappa(1+\cos\theta_0)^2 > (\ell-1)(n-\ell-1) - (n-1)\cos^2\theta_0.$$

This holds if and only if the inequality is satisfied for $\ell = [n/2]$, which is equivalent to $\kappa > \kappa_0$.

The relative equilibrium is therefore Lyapounov stable if A is positive definite, that is if $q_{11}q_{22} - q_{12}^2 > 0$ and $q_{11} > 0$. Some lengthy computations give

$$\begin{aligned} q_{11}q_{22} - q_{12}^2 &= -\tfrac{1}{8}n^2\kappa(\kappa + n\cos\theta_0)(a\kappa - b) \\ q_{11} &= \tfrac{1}{2}n\kappa(1+\cos\theta_0)^2 + n(n-1)\cos^2\theta_0 \end{aligned}$$

where a, b are given in the theorem. Now, if $\kappa > \kappa_0$, then $q_{11} > 0$: indeed

$$q_{11} = \tfrac{1}{2}n(1+\cos\theta_0)^2(\kappa-\kappa_0) + \tfrac{1}{2}n(n-1)\cos^2\theta_0 + \tfrac{n}{2}\left[\tfrac{(n-2)^2}{4}\right].$$

We proved therefore that this RE is Lyapounov stable if $\kappa > \kappa_0$ and $\kappa(\kappa+n\cos\theta_0)(a\kappa - b) < 0$.

(ii) We now study the spectral stability of the relative equilibrium. It follows from Proposition 6.1 and the block diagonalization of $\mathsf{d}^2 H_\xi|_{\mathcal{N}}(x_e)$ that

$$L_{\mathcal{N}} = \operatorname{diag}\left(A_L, \left\{\begin{pmatrix} 0 & -\lambda_\phi^{(\ell)} \\ \lambda_\theta^{(\ell)} & 0 \end{pmatrix}, \begin{pmatrix} 0 & -\lambda_\phi^{(\ell)} \\ \lambda_\theta^{(\ell)} & 0 \end{pmatrix} \mid 2 \le \ell \le [n/2]\right\}^*\right)$$

where the blocks are given up to a positive scalar factor and

$$A_L = \begin{pmatrix} 0 & 0 & a & b \\ 0 & 0 & c & d \\ -a & -b & 0 & 0 \\ -c & -d & 0 & 0 \end{pmatrix}, \quad \text{where} \begin{cases} a &= \beta q_{11} - \gamma q_{12} \\ b &= \beta q_{12} - \gamma q_{22} \\ c &= \alpha q_{12} - \gamma q_{11} \\ d &= \alpha q_{22} - \gamma q_{12} \end{cases}$$

and

$$\begin{aligned} \alpha &= -\tfrac{4\cos\theta_0}{n(\kappa+n\cos\theta_0)\sin^2\theta_0} \\ \beta &= \tfrac{1}{(\kappa+n\cos\theta_0)\sin^2\theta_0} \\ \gamma &= -\tfrac{2}{n(\kappa+n\cos\theta_0)\sin^2\theta_0}. \end{aligned}$$

These (α, β and γ) arise from $L = J\mathsf{d}^2 H_\xi$, where J is the inverse of the matrix of the symplectic form whose coefficients are given in (6.1).

The eigenvalues (up to a positive factor) of $L_{\mathcal{N}}$ are therefore

$$\pm\frac{1}{\sqrt{2}}\sqrt{\sigma \pm \sqrt{\nu}}\,, \left\{\pm \mathsf{i}\sqrt{\lambda_\theta^{(\ell)}\lambda_\phi^{(\ell)}} \mid 2 \le \ell \le [n/2]\right\}^*$$

where $\nu = a^4 + 4a^2bc - 2a^2\mathsf{d}^2 + 4bc\mathsf{d}^2 + d^4 + 8adbc$ and $\sigma = -a^2 - 2bc - \mathsf{d}^2$. The eigenvalues $\pm i\sqrt{\lambda_\theta^{(\ell)}\lambda_\phi^{(\ell)}}$ are all purely imaginary if and only if $\kappa > \kappa_0$. After some lengthy but straightforward computations we obtain that

$$\begin{aligned} \sigma &= \tfrac{1}{8\sin^2\theta_0}\big[4(1+z)^2(nz-n+2)\kappa \\ &\qquad -n^2z^4 + 4n(n-1)z^3 - 2(3n^2-8n+4)z^2 - 4n(n-1)z - n^2\big] \\ \nu &= -\tfrac{9}{16\sin^4\theta_0}\left[8(1+z)^2(nz-n+2)\kappa - \big(n(1-z^2)+4(n-1)z\big)^2\right] \end{aligned}$$

where $z = \cos\theta_0$. One can check that if $\nu \ge 0$, then $\sqrt{\nu}+\sigma \le 0$ and the eigenvalues are purely imaginary. If $\nu < 0$, then the eigenvalues have a non-zero real part. Thus the eigenvalues $\pm\sqrt{\sigma \pm \sqrt{\nu}}$ are purely imaginary if and only if $\nu \ge 0$ which is equivalent to $8a\kappa \le (n\sin^2\theta_0 + 4(n-1)\cos\theta_0)^2$. □

A spectrally stable relative equilibrium for which the Hessian $\mathsf{d}^2 H_\xi|_{\mathcal{N}}(x_e)$ is not definite is said to be *elliptic*. Note that in principle an elliptic relative equilibrium may be Lyapounov stable, but if there are more than 4 vortices then it is expected to be unstable as a result of Arnold diffusion. Moreover an elliptic relative equilibrium typically becomes linearly unstable when some dissipation is added to the system [8]; however adding dissipation to the point vortex system would have more profound effects, such as spreading of vorticity into vortex patches.

Corollary 6.3. *A $\mathbf{C}_{nv}(R,p)$ relative equilibrium with $n \geq 4$ and $\mu \neq 0$ is elliptic if and only if*

$$\kappa \geq \kappa_0, \quad \kappa(\kappa + n\cos\theta_0)(a\kappa - b) \geq 0 \quad \textit{and} \quad 8a\kappa \leq (n\sin^2\theta_0 + 4(n-1)\cos\theta_0)^2,$$

where a, b and κ_0 are given in (6.2).

Discussion of results for $n \geq 4$ See Figure 6.1.

- If the sign of the vorticity of the polar vortex is opposite to that of the ring then there are stable configurations only for $n \leq 6$. Conversely configurations with $n \leq 6$ and θ_0 close to π, ie with the ring close to the opposite pole, are Lyapounov stable for all $\kappa < 0$.
- The region of Lyapounov stability is larger when the vorticities of the pole and the ring have the same sign ($\kappa > 0$). The stability frontiers in the upper-left corners of Figure 6.1 go to infinity as θ_0 approaches $\arccos(1-2/n)$. It follows that for $n \geq 4$ and $\theta_0 > \arccos(1-2/n)$, the relative equilibria are Lyapounov stable for all sufficiently large κ. Thus, a ring of vortices is stabilized by a polar vortex with a sufficiently large vorticity of the same sign as the vortices in the ring. Note that for $4 \leq n \leq 6$ and κ positive, but sufficiently small, a ring near the opposite pole is only elliptic and may not be Lyapounov stable.
- The limiting stability results for $\theta_0 = 0$, ie when the ring is close to the polar vortex, coincide with the stability of a planar n-ring plus a central vortex, see [6] and [17]. This is also true for $n = 2$ and $n = 3$.
- The stability boundary where $\kappa = \kappa_0$ corresponds to the mode $\ell = [n/2]$ and is analogous to the stability boundary for a single ring. When n is even stability is probably lost through a pitchfork bifurcation to a relative equilibrium of type $\mathbf{C}_{\frac{n}{2}v}(R, R', p)$ consisting of two staggered $\frac{n}{2}$-rings and a pole as (κ, θ_0) passes through this boundary. This is illustrated for $n = 4$ in Figure 8 of [19], where branch (g) meets branch (d). When n is odd there is an analogous transcritical bifurcation to relative equilibria with only a single reflexional symmetry which fixes two vortices and permutes the others. These are denoted by $\mathbf{C}_h(\frac{n-1}{2}R, 2E)$ in [19]. A nice illustration in the case $n = 3$ can be found in Figure 8 of [5]. We have not checked the non-degeneracy conditions for these bifurcations.
- The $\ell = 1$ mode is responsible for two types of bifurcation. See Section 4 for descriptions of the associated bifurcations.

  Firstly, when the eigenvalues become zero, the kernel is a single irreducible symplectic representation of complex type (it is a plane with $\mathbf{C}_n$ acting by rotations) so the eigenvalues pass through zero and remain on the imaginary axis. This corresponds to a transition from Lyapounov stable to elliptic (the very thin blue (or light grey) sliver in the top left-hand corners of the figures).

  Secondly, at the other side of the blue (or light grey) sliver, the pair of eigenvalues continues to move away from 0 along the imaginary axis until it meets the other pair from the $\ell = 1$ mode; these then 'collide' and leave the imaginary axis through a Hamiltonian Hopf bifurcation.
- The transition from Lyapounov stable to elliptic when passing across the curve where $\mu = 0$ is a generic phenomenon, and can be explained by the geometry of the reduced spaces, and occurs when the RE with zero momentum is in fact an orbit of equilibria. See [26] for details.

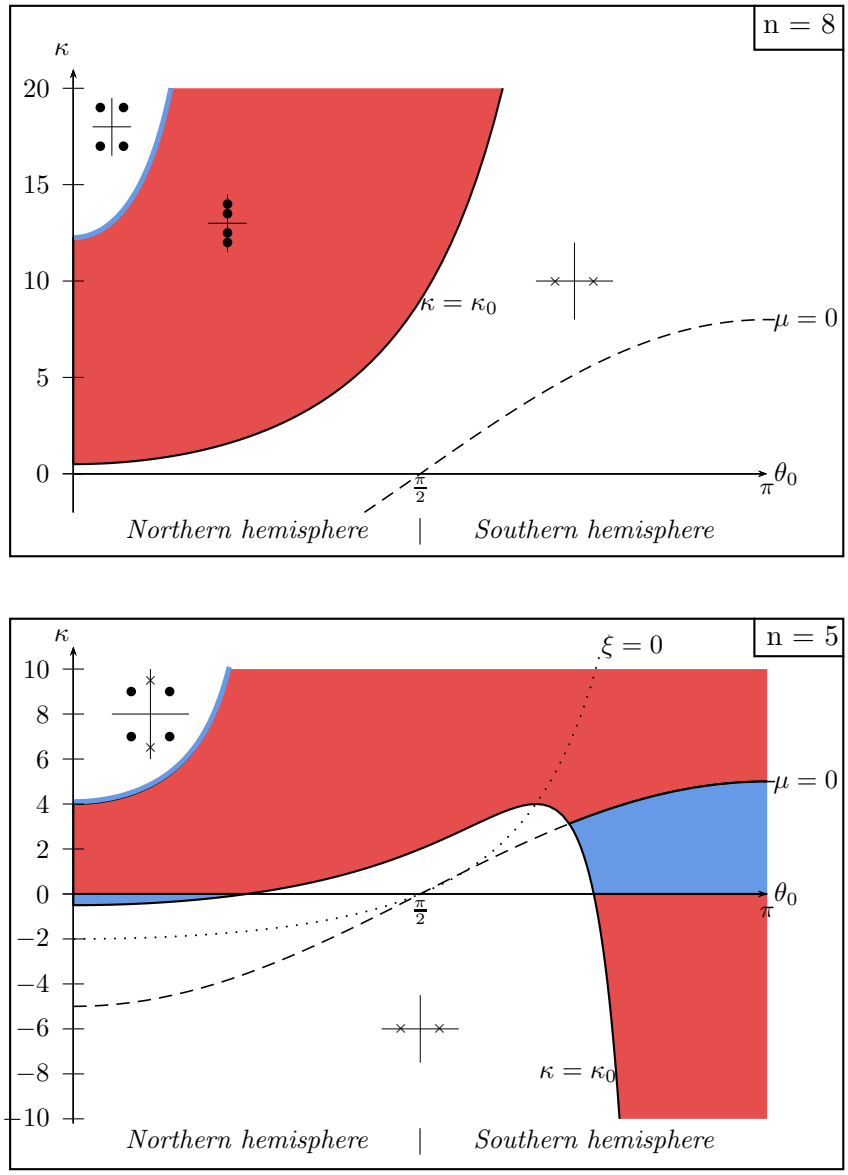

FIGURE 6.1. Bifurcation diagrams for $\mathbf{C}_{nv}(R,p)$ relative equilibria. See Fig. 6.2 for the key. The bifurcation diagrams for $n \geq 7$ are similar to that for $n = 8$, while those for $n = 4$ and 6 are similar to that for $n = 5$. The circles represent the eigenvalues of the mode $\ell = 1$, while the crosses represent those of the mode $[n/2]$. Notice the sliver of elliptic near the upper left hand corner of both diagrams: these are not drawn to scale as they are too thin—cf. Fig. 6.2 ($n = 3$), where it is drawn to scale. Stability is modulo rotations about the vertical axis (i.e., $\mathsf{SO}(2)$), or modulo all rotations if $\mu = 0$. See text for more details. In the stable regions all eigenvalues are imaginary.

- Finally we note that when κ crosses zero, eigenvalues change sign without strictly passing through zero due to the fact that the symplectic form becomes degenerate for $\kappa = 0$.
- There are other bifurcations which do not involve loss of stability, as they occur in one particular mode, while the relative equilibrium is already unstable because of a different mode. For example, for $n = 4$ and 5 (and perhaps others) there is an inverted parabola in the $\kappa < 0$ region along which there is a Hamiltonian Hopf bifurcation in the $\ell = 1$ mode (similar to that for $n = 3$ below).

Discussion of the case $n = 3$ See Figure 6.2.

Suppose first that the relative equilibrium has non-zero momentum. For $n = 3$ (so 4 vortices altogether), by the proof of Theorem 6.2 we have $\mathsf{d}^2 H_\xi|_{\mathcal{N}}(x_e) = \mathrm{diag}(A, A)$ and $L_N = A_L$. Hence $\mathbf{C}_{3v}(R, p)$ is Lyapounov stable if $\kappa(\kappa + 3\cos\theta_0)(a\kappa - b) < 0$, and spectrally unstable if and only if

$$8a\kappa > (3\sin^2\theta_0 + 8\cos\theta_0)^2,$$

where $a = (3\cos\theta_0 - 1)(1 + \cos\theta_0)^2$ as in Theorem 6.2. These results are illustrated in Figure 6.2.

- Notice that a polar vortex *destabilizes* a 3-ring if either the polar vortex is in the same hemisphere as the ring and has a sufficiently strong vorticity of the same sign as the ring, or the polar vortex has the opposite sign vorticity and the ring lies in an interval containing $\theta_0 = 2\pi/3$ that grows as the magnitude of the polar vorticity increases. These two regions have a vertical asymptote at $\cos\theta_0 = 1/3$ determined by the vanishing of a.
- Outside these regions there is a patchwork of regimes in which the relative equilibrium is either Lyapounov stable or elliptic.
- The relative equilibria with $\mu = 0$ have a 2-dimensional symplectic slice, and are all Lyapounov stable. The transition point where $\mu = \xi = 0$, $\kappa = 1$ and $\cos(\theta_0) = -1/3$ corresponds to the stable equilibrium consisting of 4 identical vortices placed at the vertices of a regular tetrahedron [39, 19, 14].
- Comparing this case with the diagram for $n = 5$ shows large regions of stability with $\kappa < 0$ which are unstable for $n = 5$. The instability for $n = 5$ is due to the $\ell = 2$ mode which is absent for $n = 3$.

Discussion of the case $n = 2$ See Figure 6.2.

The $\mathbf{C}_{2v}(R, p)$ relative equilibria are isosceles triangles lying on a great circle, and for $\theta_0 = 2\pi/3$ the triangle becomes equilateral. We again discuss the stability of those with non-zero momentum. Indeed, any 3-vortex configuration with zero momentum is a relative equilibrium since the reduced space is just a point, and is consequently also Lyapounov stable relative to $\mathsf{SO}(3)$ [36].

For $n = 2$ the symmetry adapted basis for V_1 is

$$\begin{aligned} e_1 &= \kappa\, \alpha_\theta^{(1)} + 2\cos\theta_0\, \delta x, \\ e_2 &= \kappa\, \alpha_\phi^{(1)} + 2\sin\theta_0\, \delta y. \end{aligned}$$

with $\omega(e_1, e_2) = 2\kappa\sin\theta_0\,(2\cos\theta_0 + \kappa)$ (which vanishes only when $\mu = 0$). Following the proof of Theorem 6.2 we obtain

$$\mathsf{d}^2 H_\xi^{(1)} = 2\kappa\mu \begin{pmatrix} \frac{\kappa(1+\cos\theta_0)^2 + 3\cos^2\theta_0 + 2\cos\theta_0}{\sin^2\theta_0} & 0 \\ 0 & -(1 + 2\cos\theta_0) \end{pmatrix}.$$

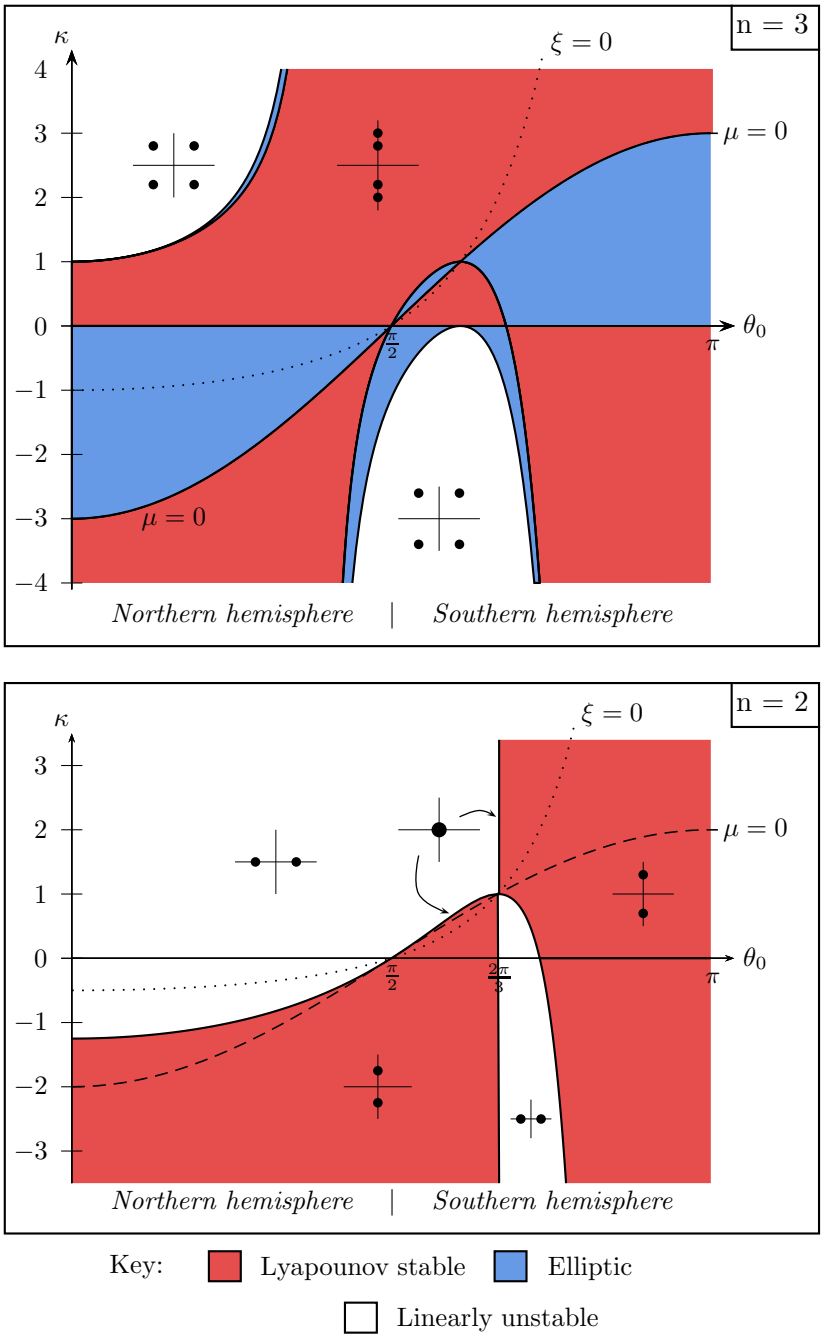

FIGURE 6.2. Bifurcation diagrams for $\mathbf{C}_{3v}(R,p)$ and $\mathbf{C}_{2v}(R,p)$ relative equilibria (so a total of 4 and 3 vortices respectively); the polar vortex of strength κ is at the North pole. Stability is modulo $\mathsf{SO}(2)$ about the polar axis, or modulo $\mathsf{SO}(3)$ when $\mu = 0$ (see text). The circles represent the eigenvalues of the mode $\ell = 1$.

Consequently, for $\mu \neq 0$, the $\mathbf{C}_{2v}(R,p)$ relative equilibrium is Lyapounov stable if this matrix is definite, so if

$$(1+2\cos\theta_0)[(1+\cos\theta_0)^2\kappa+\cos\theta_0(2+3\cos\theta_0)]<0.$$

It is spectrally unstable if the inequality is reversed. See Figure 6.2.

- There are two stable regions. For $\theta_0 < 2\pi/3$ the relative equilibria are stable provided the polar vorticity is less than a certain θ_0 dependent critical value, while for $\theta_0 > 2\pi/3$ they are stable for all polar vorticities greater than a critical value. As $\theta_0 \to \pi$ this value goes to $-\infty$.
- For $\theta_0 = \pi/2$, where the 2-ring is equatorial and the isosceles triangle is right-angled, they are stable if and only if $\kappa < 0$. This is in agreement with [39, Theorem III.3], with $\Gamma_1 = \Gamma_2 = 1$, and $\Gamma_3 = \kappa$.
- *The restricted three vortex problem* The range of stability when $\kappa = 0$ does not coincide with the range of stability for a single ring. Indeed the $\mathbf{C}_{2v}(R)$ relative equilibria are Lyapounov stable for all co-latitudes (see Theorem 5.2) while $\mathbf{C}_{2v}(R,p)$ is unstable for $\kappa = 0$ and $\theta_0 \in (0,\pi/2)$. This means that if we place a *passive tracer* or *ghost vortex* at the North pole and a ring of two vortices in the Northern hemisphere, then the passive tracer will be unstable.

Remark 6.4. The stability of $\mathbf{C}_{nv}(R,p)$ relative equilibria has also been studied in [5]. However our method differs significantly from theirs in that we consider the definiteness of the Hessian $\mathsf{d}^2 H_\xi|_{\mathcal{N}}(x_e)$ on the $2n-2$ dimensional symplectic slice, while in [5] the authors determine conditions for the Hessian to be definite on the whole $2n+2$ dimensional tangent space. The result is that we prove the relative equilibria to be Lyapounov stable in a larger region of the parameter space. Notice in particular that for $n \leq 6$ our results say that a positive vorticity n-ring near the South pole is Lyapounov stable if the North pole has either negative or sufficiently positive vorticity. However in [5] only the case of negative North polar vorticity is shown to be Lyapounov stable. In this paper we also give criteria for when the relative equilibria are *unstable* by considering the eigenvalues of the linearization $L_{\mathcal{N}}$.

7. **Two aligned rings: $\mathbf{C}_{nv}(2R)$.** In this section we consider relative equilibria x_e of symmetry type $\mathbf{C}_{nv}(2R)$, that is configurations formed of two 'aligned' rings of n vortices each as illustrated in Figure 1.2. We can assume without loss of generality that the vorticities of the vortices in the first and second ring are 1 and κ, respectively, and we denote their co-latitudes by θ_1 and θ_2. We can also assume that the ring of vorticity 1 and co-latitude θ_1 lies in the Northern hemisphere, $\theta_1 \in (0,\pi/2]$. The first question to answer is, *for which values of the parameters* $(\theta_1,\theta_2,\kappa)$ *is the configuration* $\mathbf{C}_{nv}(2R)$ *a relative equilibrium?* It was shown in [19] (p. 126) that for given $\kappa > 0$ and each μ with $|\mu| < n|1+\kappa|$ there is at least one solution for (θ_1,θ_2) with $n\cos\theta_1 + n\kappa\cos\theta_2 = \mu$ and with $\theta_1 < \theta_2$ and at least one with $\theta_2 < \theta_1$. We now make this more precise.

The isotropy subgroup G_{x_e} is the dihedral group $\mathbf{C}_{nv}$. The fixed point set $\mathrm{Fix}(G_{x_e})$ consists of all pairs of aligned rings, with one vortex from each ring on a given meridian, so can be parametrized by $x := \cos\theta_1$ and $y := \cos\theta_2$. Denote by $\tilde{F}$ the restriction of a function F to $\mathrm{Fix}(G_{x_e})$. The Hamiltonian can be split in such a way that

$$H \;=\; H_{11} + \kappa H_{12} + \kappa^2 H_{22}$$

where H_{11}, H_{12}, H_{22} do not depend on κ, $\tilde{H}_{11}$ does not depend on y and $\tilde{H}_{22}$ does not depend on x (H_{11} governs the interactions within the first ring, H_{12} the interactions between the rings etc). The following proposition shows that for almost every pair (θ_1, θ_2) there exists a unique κ such that the $\mathbf{C}_{nv}(2R)$ configuration with parameters $(\theta_1, \theta_2, \kappa)$ is a relative equilibrium.

Proposition 7.1. *Let x_e be a $\mathbf{C}_{nv}(2R)$ configuration with parameters $(\theta_1, \theta_2, \kappa)$.*

1. *There exists a unique $\kappa \in \mathbb{R}^*$ such that x_e is a relative equilibrium if and only if both the following conditions hold:*

$$\left(\frac{\partial \tilde{H}_{12}}{\partial y} - \frac{\partial \tilde{H}_{11}}{\partial x}\right)(\cos\theta_1, \cos\theta_2) \neq 0, \quad \left(\frac{\partial \tilde{H}_{22}}{\partial y} - \frac{\partial \tilde{H}_{12}}{\partial x}\right)(\cos\theta_1, \cos\theta_2) \neq 0.$$

2. *The configuration x_e is a relative equilibrium for all $\kappa \in \mathbb{R}^*$ in the degenerate case when both the following conditions hold:*

$$\left(\frac{\partial \tilde{H}_{12}}{\partial y} - \frac{\partial \tilde{H}_{11}}{\partial x}\right)(\cos\theta_1, \cos\theta_2) = 0, \quad \left(\frac{\partial \tilde{H}_{22}}{\partial y} - \frac{\partial \tilde{H}_{12}}{\partial x}\right)(\cos\theta_1, \cos\theta_2) = 0.$$

In both cases the angular velocity ξ of x_e satisfies

$$\xi \;=\; \frac{1}{n}\left(\frac{\partial \tilde{H}_{11}}{\partial x}(x_e) + \kappa \frac{\partial \tilde{H}_{12}}{\partial x}(x_e)\right).$$

The sign of κ as a function of θ_1, θ_2 is shown in Figure 7.1.

Proof. Since $H - \xi\Phi$ is a G_{x_e}-invariant function (see Section 2) the Principle of Symmetric Criticality [35] implies that x_e is a relative equilibrium if and only if it is a critical point of $\tilde{H} - \xi\tilde{\Phi}$. It follows from $\tilde{\Phi} = n(x + \kappa y)$ that $\mathsf{d}(\tilde{H} - \xi\tilde{\Phi})(x_e) = 0$ is equivalent to the pair of equations:

$$\kappa\left(\frac{\partial \tilde{H}_{22}}{\partial y}(x_e) - \frac{\partial \tilde{H}_{12}}{\partial x}(x_e)\right) + \frac{\partial \tilde{H}_{12}}{\partial y}(x_e) - \frac{\partial \tilde{H}_{11}}{\partial x}(x_e) \;=\; 0$$

$$\xi = \frac{1}{n}\left(\frac{\partial \tilde{H}_{11}}{\partial x}(x_e) + \kappa \frac{\partial \tilde{H}_{12}}{\partial x}(x_e)\right).$$

The proposition follows easily from these. □

For example, in the case $n = 4$ the degenerate case occurs when the two rings form the vertices of a cube. Hence for any values of the vorticities of the two rings the 'cube configuration' is a relative equilibrium. However among this family of relative equilibria only one is an equilibrium, namely the one for which the two rings have the same vorticities, $\kappa = 1$, which corresponds to the $\mathbb{O}_h(f)$ equilibrium of [19], a cube formed of identical vortices, and which is known to be unstable [14]. In Figure 7.1, the cubic configurations are marked by two dots. For $n = 2$, the degenerate case occurs when the vortices form a square lying on a great circle.

For $\theta_2 = \pi - \theta_1$, the configuration has an extra symmetry and its symmetry type is $D_{nh}(2R)$. Such a configuration is a relative equilibrium if the two rings have opposite vorticities ($\kappa = -1$). The existence and stability of such relative equilibria were studied in [15].

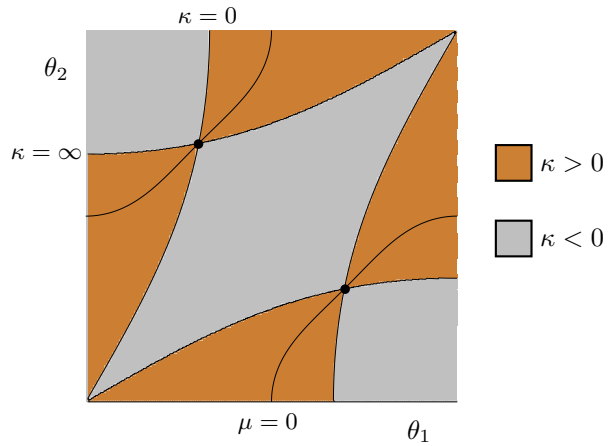

FIGURE 7.1. Sign of κ for $\mathbf{C}_{nv}(2R)$ relative equilibria. The degenerate case occurs where the curves $\kappa = 0$ and $\kappa = \infty$ intersect. The figure is for $n = 4$, but is similar for other values of n. The only region of stability (see Fig. 7.2) lies at the bottom right hand and top left-hand corners, corresponding to the rings lying far apart in opposite hemispheres, and is contained in the region $\kappa < 0$. Along both diagonals (where $\theta_1 = \theta_2$ and $\theta_1 + \theta_2 = \pi$) one has $\kappa = -1$. The two black curves are where $\mu = 0$. Note that reflecting along either diagonal exchanges the rings, so corresponds to changing κ to κ^{-1}.

With the help of the discussion of Section 3.3, one can perform a G_{x_e}-invariant isotypic decomposition and find that the symmetry adapted basis for the symplectic slice at a $\mathbf{C}_{nv}(2R)$ relative equilibrium with $n \geq 3$ and $\mu \neq 0$ is

$$\left(e_1, e_2, f_1, f_2, f_3, f_4, f_5, f_6, B_2, B_3, \ldots, B_{[n/2]}\right)$$

where

$$\begin{aligned} e_1 &= \alpha^{(0)}_{0,\phi} - \alpha^{(0)}_{1,\phi} \\ e_2 &= \kappa \sin\theta_2 \; \alpha^{(0)}_{0,\theta} - \sin\theta_1 \; \alpha^{(0)}_{1,\theta} \end{aligned}$$

$$\begin{aligned} f_1 &= \sin\theta_1 \; \alpha^{(1)}_{0,\theta} + \cos\theta_1 \; \beta^{(1)}_{0,\phi} & f_2 &= \sin\theta_2 \; \alpha^{(1)}_{1,\theta} + \cos\theta_2 \; \beta^{(1)}_{1,\phi} \\ f_3 &= \kappa \sin\theta_2 \; \beta^{(1)}_{0,\phi} - \sin\theta_1 \; \beta^{(1)}_{1,\phi} & f_4 &= \cos\theta_1 \; \alpha^{(1)}_{0,\phi} - \sin\theta_1 \; \beta^{(1)}_{0,\theta}, \\ f_5 &= \cos\theta_2 \; \alpha^{(1)}_{1,\phi} - \sin\theta_2 \; \beta^{(1)}_{1,\theta} & f_6 &= \kappa \sin\theta_2 \; \alpha^{(1)}_{0,\phi} - \sin\theta_1 \; \alpha^{(1)}_{1,\phi} \end{aligned}$$

and,

$$\begin{aligned} B_\ell &= \left\{\alpha^{(\ell)}_{0,\theta},\, \alpha^{(\ell)}_{1,\theta},\, \alpha^{(\ell)}_{0,\phi},\, \alpha^{(\ell)}_{1,\phi},\, \beta^{(\ell)}_{0,\theta},\, \beta^{(\ell)}_{1,\theta},\, \beta^{(\ell)}_{0,\phi},\, \beta^{(\ell)}_{1,\phi}\right\} \quad \text{for } 2 \leq \ell < n/2 \\ B_{n/2} &= \left\{\alpha^{(n/2)}_{0,\theta},\, \alpha^{(n/2)}_{1,\theta},\, \alpha^{(n/2)}_{0,\phi},\, \alpha^{(n/2)}_{1,\phi}\right\} \quad \text{for even } n. \end{aligned}$$

The adapted basis for $n = 2$ is simply $(e_1, e_2; f_6, f_7)$, where

$$f_7 = \kappa \cos\theta_2 \; \alpha^{(1)}_{0,\theta} - \cos\theta_1 \; \alpha^{(1)}_{1,\theta} \, .$$

Remark Almost all $\mathbf{C}_{nv}(2R)$ relative equilibria have a non-zero momentum. Indeed $\mu = 0$ if and only if $x + \kappa y = 0$, and from the expression of κ one can show that

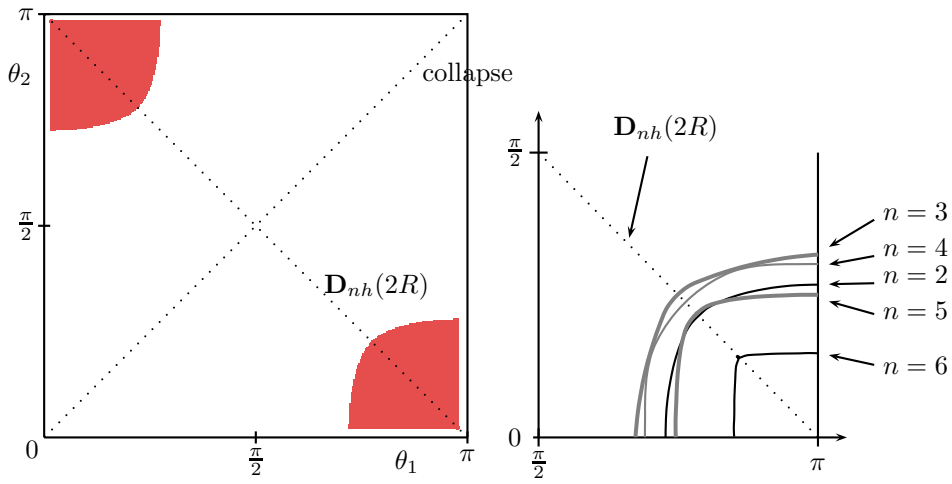

FIGURE 7.2. Stability results for $\mathbf{C}_{nv}(2R)$ relative equilibria; that is for two aligned rings. The coloured regions in the left-hand diagram represents the configurations that are Lyapounov stable. The figure is for $n = 2$, but is very similar for $n \leq 6$. The right-hand figure illustrates the different sizes of the stable regime for the different values of n. If n is odd there is a narrow strip (too narrow to discern on this diagram) between the Lyapounov stable and the linearly unstable configurations where the relative equilibria are elliptic. For $n \geq 7$, it seems that all relative equilibria are unstable.

this last equation defines an algebraic curve in variables $(x, y) \in [0, 1) \times (-1, 1) \simeq \operatorname{Fix} \mathbf{C}_{nv}$ (depicted in Figure 7.1). Numerics suggest that equilibria ($\xi = 0$) occur along curves that are extremely close to these momentum zero curves, and indeed would be indistinguishable in the diagram.

With respect to this basis $\mathsf{d}^2 H_\xi|_{\mathcal{N}}(x_e)$ block diagonalizes into: two 1×1 blocks for $\ell = 0$, two 3×3 blocks for $\ell = 1$, two 4×4 blocks for each of $\ell = 2 \ldots [(n-1)/2]$), together with two 2×2 blocks for $\ell = n/2$ when n is even. The linearization $L_{\mathcal{N}}$ block diagonalizes into half as many blocks of twice the size. In order to calculate the stability of the relative equilibria, we ran a MAPLE program to compute numerically the eigenvalues of each of the blocks of $\mathsf{d}^2 H_\xi|_{\mathcal{N}}(x_e)$ and $L_{\mathcal{N}}$. The results are summarized for $n = 2 \ldots 6$ in Figure 7.2. Figure 7.1 shows how the sign of κ varies for relative equilibria with different values of θ_1 and θ_2. A selection of the MAPLE code is available for download from [27]; further diagrams are also available from the same site.

Discussion of results Here we outline conclusions from a series of numerical calculations, using MAPLE. These involved calculating eigenvalues of the Hessian matrix and the linearization using the Fourier bases described above, varying the co-latitudes θ_1 and θ_2 across the range 0 to π in steps of 10^{-2} (and occasionally smaller steps to investigate specific bifurcations).

- These numerical calculations suggest strongly that the relative equilibria $\mathbf{C}_{nv}(2R)$ are never stable if the two rings lie in the same hemisphere (Figure 7.2) or have the same sign vorticity (Figure 7.1).
- The stable configurations are for one ring close to the North pole and the other ring close to the South pole, and always with vorticity of opposite signs. For $n = 4$, the furthest from the poles both rings can be is about $40°$ of latitude. This is in agreement with Theorem 4.8 of [15].
- For $n > 2$, as n increases the region of stability decreases in size. Numerical experiments with $n \geq 7$ suggest that in these cases the relative equilibria are never stable.
- The stability boundaries for $2 \leq n \leq 6$ approach configurations where one ring is at a pole and the other lies at a particular co-latitude θ_z in the opposite hemisphere. For $n = 3, 4$, $\theta_z \approx 0.95\text{rad} \approx 55°$, for $n = 2, 5$, $\theta_z \approx 0.8\text{rad} \approx 46°$, and for $n = 6$, $\theta_z \approx 0.45\text{rad} \approx 25°$.
- For $n = 2$, 4 and 6 stability is first lost by a pair of imaginary eigenvalues of the $\ell = n/2$ block of $L_{\mathcal{N}}$ passing through 0 and becoming real (the 'splitting' case described in Section 4). The difference between even and odd n (see next point) is that the type of representation on the $\ell = n/2$ mode is 'of real type'.
- For $n = 3$ and 5 a pair of imaginary eigenvalues of the $\ell = (n-1)/2$ block passes through 0 but remains on the imaginary axis, so the stability changes from Lyapounov to elliptic (the 'passing' case described in Section 4). This imaginary pair then collides with another pair, and all move off the imaginary axis to form a complex quadruplet and create instability (a Hamiltonian Hopf bifurcation). However, the elliptic regions are very narrow: for $n = 3$ with $\theta_1 = 0.1$ the elliptic region is contained in $|\theta_2 - 2.1438318| < 10^{-7}$. For $\theta_2 = \pi - \theta_1$ (the $\mathbf{D}_{nh}(2R)$ configurations) the elliptic range is at its widest, but is still only approximately $|\theta_2 - 0.777| < 6 \times 10^{-3}$, which is too small to be seen in Figure 7.2. For $n = 5$ the elliptic region is even narrower.
- As (θ_1, θ_2) approaches the diagonal (that is, the rings approach one another) so $\kappa \to -1$, and the configuration approaches one of n dipoles (pairs with equal and opposite vorticities).
- When $\kappa = 0$ (or $\kappa^{-1} = 0$) the system is not Hamiltonian, as the symplectic form is degenerate, and since we are using Hamiltonian methods further work would be needed to find the stability at these points.

8. **Two staggered rings: $\mathbf{C}_{nv}(R, R')$.** In this section we consider relative equilibria formed of two rings of n vortices each of strengths 1 and κ and co-latitude θ_1 and θ_2 respectively. They differ from those of the previous section in that the rings here are 'staggered', that is they rotated relative to each other with an offset of π/n. Their symmetry type is $\mathbf{C}_{nv}(R, R')$. As in the previous section we can assume without loss of generality that the ring of vorticity 1 and co-latitude θ_1 lies in the Northern hemisphere. The difference between the stabilities of aligned and staggered rings is striking: compare Figures 7.2 and 8.2.

Proposition 7.1 also holds for $\mathbf{C}_{nv}(R, R')$ configurations: for almost every pair (θ_1, θ_2) there exists a unique κ such that the corresponding $\mathbf{C}_{nv}(R, R')$ configuration is a relative equilibrium, and κ, ξ are given by the same expressions in terms of the derivatives of $\tilde{H}_{ij}$. The only difference from Section 7 is the expression for $\tilde{H}_{12}$ in terms of θ_1 and θ_2 (or x and y).

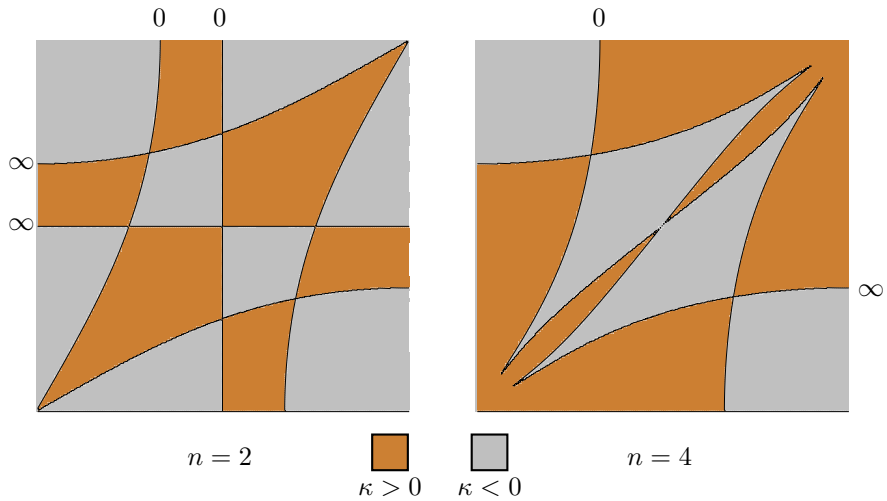

FIGURE 8.1. Sign of κ for $\mathbf{C}_{nv}(R, R')$ relative equilibria for $n = 2$ and 4. The diagrams for $n \geq 3$ are all similar, with the central strip where $\kappa > 0$ getting thinner as n increases. See the discussion of results below for more details.

When $\theta_2 = \theta_1$ the configuration forms a single ring with $2n$ vortices with $\kappa = 1$: all the vortices have the same vorticity. These are the relative equilibria of type $\mathbf{C}_{2nv}(R)$ studied in Section 3.2. For $\theta_2 = \pi - \theta_1$, the configuration has an extra symmetry and its symmetry type is $D_{nd}(R, R')$. In this case $\kappa = -1$, the two rings have opposite vorticities. The existence and stability of such relative equilibria were studied in [15].

There exist also degenerate cases in the sense of Proposition 7.1. For $n = 2$ these are, a square on a great circle which is a relative equilibrium whenever the opposite vortices have the same vorticity and the tetrahedral configuration, which is shown in [39] to be a relative equilibrium for any values of the four vorticities. These are discussed further below.

With the help of the discussion of Section 3.3, one finds that a symmetry adapted basis for the symplectic slice at a $\mathbf{C}_{nv}(R, R')$ relative equilibrium with $n \geq 3$ and $\mu \neq 0$ is given by:

$$\left(e_1, e_2, e_3, e_4, e_5, e_6, e_7, e_8, B_2, B_3, \ldots, B_{[n/2]}\right)$$

for n odd, while for n even one is given by:

$$\begin{aligned}(e_1, e_2, e_3, e_4, e_5, e_6, e_7, e_8, \{B_\ell \mid 2 \leq \ell \leq n/2 - 1\}, \\ \alpha_{0,\theta}^{(n/2)} - \alpha_{1,\theta}^{(n/2)}, \alpha_{0,\phi}^{(n/2)} - \alpha_{1,\phi}^{(n/2)}, \beta_{1,\theta}^{(n/2)}, \beta_{1,\phi}^{(n/2)}\Big),\end{aligned}$$

where the expressions of $e_1, \ldots, e_8$ and B_ℓ remain as in the previous section. The corresponding symmetry adapted basis for $n = 2$ is simply (e_1, e_2, e_3, e_6). As in the previous section, it can readily be seen that almost all $\mathbf{C}_{nv}(R, R')$ relative equilibria have non-zero momenta.

As for the aligned rings, we ran a MAPLE program to determine the stability of the relative equilibria. The results are summarized in Figure 8.2 for n from 2 to 6.

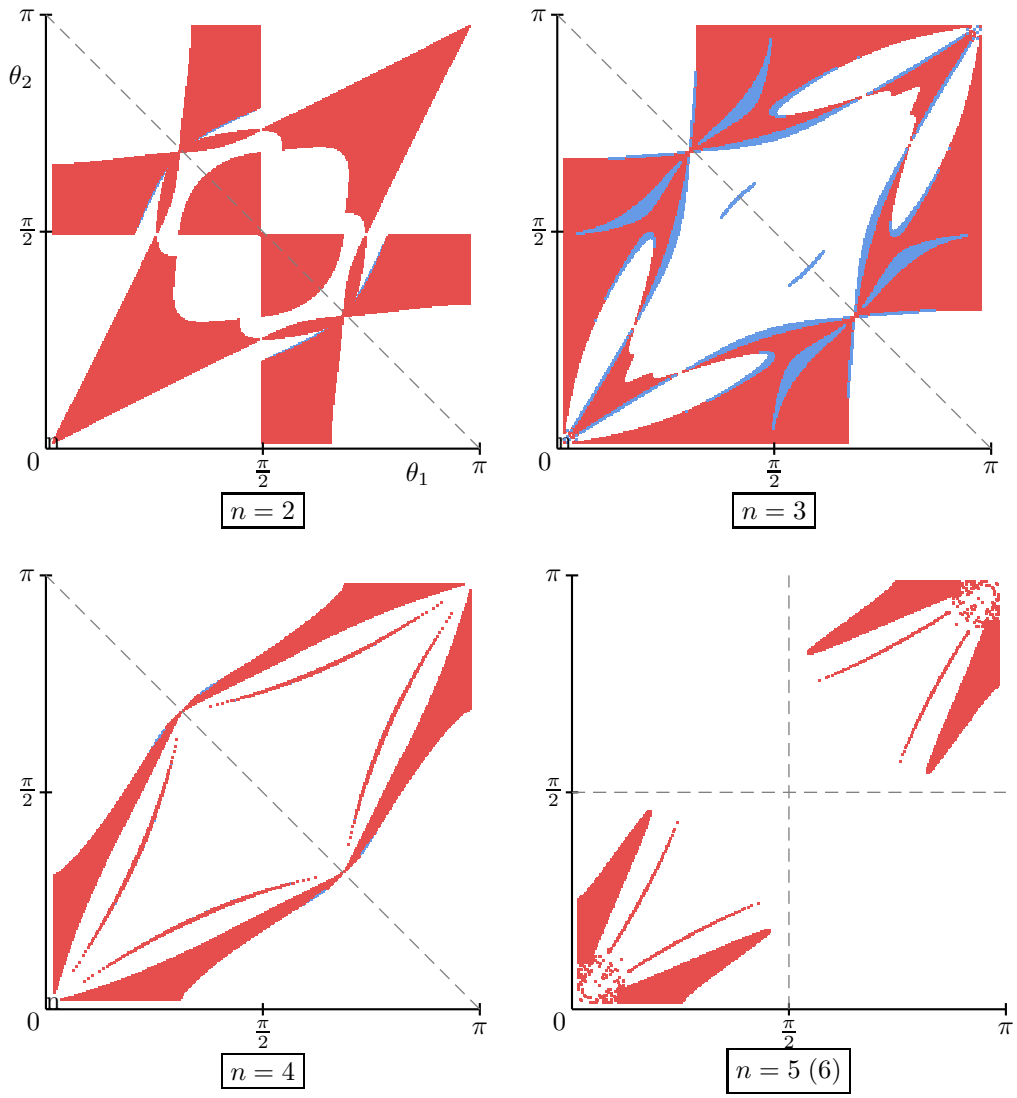

FIGURE 8.2. Stability results for two staggered rings with n identical vortices in each (the $\mathbf{C}_{nv}(R, R')$ relative equilibria). See Figure 6.2 for the meaning of the colours. The diagram for $n = 6$ (two rings with 6 vortices in each) is very similar to that for $n = 5$, but with a smaller region of stability (reduced by about 70%). For $n \geq 7$, it seems that the relative equilibria are all unstable. The diagonal dashed lines represent configurations with $\theta_2 = \pi - \theta_1$, where $\kappa = -1$; the $\mathbf{D}_{nd}(R, R')$ configurations of [15]. The figures are produced using MAPLE, where the entire square is scanned with a step-size of 10^{-2}, so nearly 10^5 data points in each diagram.

Discussion of results

- Referring first to Figure 8.1, the diagonal $\theta_1 = \theta_2$ corresponds to a single ring with $2n$ vortices, so must allow $\kappa = 1$ for all n; for $n \geq 3$ the two interior grey regions appear to extend to the corners of the square, so that for all n there are relative equilibria close to the poles with all possible values of κ. Each curve is labeled with a 0 or an ∞, corresponding to the 'value' of κ along that curve. The degenerate case occurs where the curves $\kappa = 0$ and $\kappa = \infty$ intersect. (Note that rotating the diagram by π corresponds to turning the sphere upside down, which is a symmetry of the system and so preserves the value of κ.)
- Numerical experiments suggest that stable relative equilibria only exist for $n \leq 6$.
- Refer now to Figure 8.2. For $n = 5$ and 6 the relative equilibria $\mathbf{C}_{nv}(R, R')$ are stable only if the two rings lie in the same hemisphere but are sufficiently far apart.
- For $n \leq 4$ these stable regions extend to include relative equilibria with the rings in different hemispheres. However, contrary to the case $\mathbf{C}_{nv}(2R)$, the stable regions are far from the line $\theta_2 = \pi - \theta_1$ corresponding to $\mathbf{D}_{nd}(R, R')$ relative equilibria.
- For $n = 2$ and 3 there is also a stable region with the two rings in the same hemisphere and close to each other. This includes the stable $\mathbf{C}_{4v}(R)$ and $\mathbf{C}_{6v}(R)$ relative equilibria discussed in Section 3.2.
- Note also that for $n \leq 6$, there exist stable relative equilibria (for some values of κ) in any neighbourhood of $(\theta_1, \theta_2) = (0, 0)$, that is with the two rings close to a pole.
- A study of the sign of κ shows that when $3 \leq n \leq 6$ the relative equilibria with $\kappa < 0$ are almost all unstable. The only ones that are not are elliptic, and occur in very narrow strips around the 'hairs' towards the diagonal in the diagrams for $n = 4, 5, 6$, and along the corresponding parts of the diagram for $n = 3$, as well as the elliptic crescents near the centre of the $n = 3$ diagram.

  However for $n = 2$ there exist relative equilibria with $\kappa > 0$ in the Lyapounov stable region corresponding to the two rings both being relatively close to the equator, but in opposite hemispheres (see also the discussion below on the tetrahedral configuration).
- It follows from Section 5 that the equatorial square is unstable if all the vorticities are equal. However, the equatorial square with opposite vortices having the same vorticity is always an equilibrium, regardless of the two values of vorticity, and always with momentum $\mu = 0$. This is the point in the centre of the first diagram in Figure 8.2. The regions of stability and instability neighbouring this central point correspond to different vorticity ratios. Since $\mu = 0$ the only relevant mode is $\ell = 0$, and the corresponding Hessian is $\mathrm{diag}[16\kappa,\ -4\kappa^2]$ so the equatorial square is (linearly and non-linearly) stable if and only if $\kappa < 0$. (This agrees with the conclusion in [15, Theorem 4.6] where the case $\kappa = -1$ is considered.)
- It is shown by Pekarsky and Marsden [39] that the tetrahedral configuration (where $\cos\theta_1 = 1/\sqrt{3} = -\cos\theta_2$) is a relative equilibrium for all values of the four vorticities, though they do not discuss the stabilities. Kurakin shows that the tetrahedral equilibrium with all 4 vortices identical is Lyapounov stable [14].

In Figure 8.2 with $n = 2$, the tetrahedral configurations lie at the two points where the two stable regions meet two unstable regions on the dashed line (but not in the centre, which corresponds to the square). In particular here we have two pairs of identical vortices (with vorticities 1 and κ) and these are relative equilibria for all values of κ. For some values these are stable, and will have the stable regions nearby, while for others they are unstable, and will have the corresponding unstable regions nearby. Simple calculations show that they are Lyapounov stable when $|\kappa + 5| > 2\sqrt{6}$ (but $\kappa \neq 0$) and linearly unstable in the remaining interval $|\kappa + 5| < 2\sqrt{6}$ (the bifurcation points are $\kappa \approx -9.9$ and -0.1).

- The analogous point with $n = 3$ corresponds to the configuration with 6 vortices lying at the vertices of an octahedron, with one ring (of unit vorticity) with $\cos\theta_1 = 1/\sqrt{3}$ forming one face, and the other ring (of vorticity κ) forming the opposite face of the octahedron, where $\cos\theta_2 = -1/\sqrt{3}$. This is a relative equilibrium for all values of κ. Kurakin [14] has shown this is stable when all vorticities are equal (the $\mathbb{O}(v)$ relative equilibrium of [19]). Calculations using Maple show that this is in fact Lyapounov stable if $\kappa > 0$. It is linearly unstable if $|\kappa + 7| < 4\sqrt{3}$, otherwise it is elliptic.
- Some of the changes in stability as θ_1, θ_2 are varied coincide with a change of sign of κ (for example, when $n = 2$ and one ring lies on the equator). As already pointed out, when $\kappa = 0$ the system is not Hamiltonian, and the methods used do not immediately apply. To our knowledge, bifurcations involving a degeneracy of the symplectic form have not been investigated.

9. **A ring with two polar vortices: $\mathbf{C}_{nv}(R, 2p)$.** In this final section we consider relative equilibria x_e of symmetry type $\mathbf{C}_{nv}(R, 2p)$; that is configurations formed of a ring of n vortices of unit strength, together with two polar vortices p_N and p_S of strengths κ_N and κ_S, respectively at the North and South poles. We may assume without loss of generality that the ring lies in the Northern hemisphere. There is thus a 3-parameter family of relative equilibria to consider: the parameters being κ_N, κ_S and either the momentum μ or the co-latitude θ_0 of the ring.

The complexity of the study in this case is increased on two counts, compared with the earlier setting of a ring with a single polar vortex: firstly there are now three parameters κ_N, κ_S and the co-latitude θ_0 of the relative equilibrium, and secondly (for $n > 2$) the $\ell = 1$ mode of the symplectic slice is of dimension 6 rather than 4. So we need to study a 3-parameter family of 3-degree of freedom systems. We proceed to obtain analytic (in)stability criteria for the relative equilibria with respect to the $\ell \geq 2$ modes, which of course give sufficient conditions for genuine instability. We then treat the remaining $\ell = 1$ mode numerically for a few low values of n. If $n = 2$ or 3 then there is only the $\ell = 1$ mode; the results for $n = 3$ are very similar to larger rings (apart from the 'cut-off' due to the higher modes when $n > 3$). On the other hand, for $n = 2$ the results are quite different, so we describe this last case separately at the end of this section.

The Hamiltonian is given by

$$H = H_r + H_{p_N} + H_{p_S} + H_{NS}$$

where H_r is given in Section 5 and

$$\begin{array}{rcl} H_{p_N} & = & -\kappa_N \sum_{i=1}^n \ln(1-\sin\theta_i\cos\phi_i\ x_N - \sin\theta_i\sin\phi_i\ y_N - \cos\theta_i\ z_N) \\ H_{p_S} & = & -\kappa_S \sum_{i=1}^n \ln(1-\sin\theta_i\cos\phi_i\ x_S - \sin\theta_i\sin\phi_i\ y_S - \cos\theta_i\ z_S) \\ H_{NS} & = & -\kappa_N\kappa_S \ln(1-x_N x_S - y_N y_S - z_N z_S), \end{array}$$

where $z_N = \sqrt{1-x_N^2-y_N^2}$ and $z_S = -\sqrt{1-x_S^2-y_S^2}$, and we have assumed the n vortices in the ring are of unit vorticity. The augmented Hamiltonian is:

$$H_\xi = H - \xi\left(\sum_{j=1}^n \cos\theta_j + \kappa_N\, z_N + \kappa_S\, z_S\right).$$

The angular velocity of the relative equilibrium x_e at $x_N = y_N = x_S = y_S = 0,\ \theta_j = \theta_0,\ \phi_j = 2\pi j/n$ is found to be

$$\xi = \frac{(n-1)\cos\theta_0 + \kappa_N(1+\cos\theta_0) - \kappa_S(1-\cos\theta_0)}{\sin^2\theta_0}.$$

The momentum for this configuration is $(0,0,\mu)$ with $\mu = \kappa_N - \kappa_S + n\cos\theta_0$, which gives

$$\xi = \frac{1}{\sin^2\theta_0}\left(\mu + (\kappa_N+\kappa_S-1)\cos\theta_0\right).$$

The second derivatives of H at the relative equilibrium can be derived from those for H_r (Section 5), those for H_p (Section 6), together with

$$\frac{\partial^2 H_{NS}}{\partial x_N^2} = \frac{\partial^2 H_{NS}}{\partial y_N^2} = \frac{\partial^2 H_{NS}}{\partial x_S^2} = \frac{\partial^2 H_{NS}}{\partial y_S^2} = \frac{\partial^2 H_{NS}}{\partial x_N \partial x_S} = \frac{\partial^2 H_{NS}}{\partial y_N \partial y_S} = \frac{1}{2}\kappa_N\kappa_S\,, \quad (9.1)$$

while the other second derivatives of H_{NS} vanish.

As in the previous sections, we can choose a symmetry adapted basis of the symplectic slice such that the matrices $\mathsf{d}^2 H_\xi|_{\mathcal{N}}(x_e)$ and $L_{\mathcal{N}}$ block diagonalize. Bases of V_ℓ for $\ell = 2,\dots\frac{n}{2}$ are given in Proposition 3.3.

Proposition 9.1. *The symplectic slice decomposes as $\mathcal{N} = \bigoplus_{\ell=1}^{[n/2]} V_\ell$, where for $\mu \neq 0$*

$$\dim V_1 = \begin{cases} 4 & \text{if } n = 2 \\ 6 & \text{if } n \geq 3. \end{cases}$$

If $\mu = 0$ the dimension of V_1 is reduced by 2.

For $n \geq 3$ and $\mu \neq 0$ a basis for V_1 is $\{e_1, e_2, \dots, e_6\}$, where

$$\begin{array}{rcl} e_1 & = & \sin\theta_0\ \alpha_\theta^{(1)} + \cos\theta_0\ \beta_\phi^{(1)} \\ e_2 & = & 2\kappa_N\ \beta_\phi^{(1)} + N\sin\theta_0\ \delta x_1 \\ e_3 & = & \kappa_S\ \delta x_1 - \kappa_N\ \delta x_2 \\ e_4 & = & \sin\theta_0\ \beta_\theta^{(1)} - \cos\theta_0\ \alpha_\phi^{(1)} \\ e_5 & = & 2\kappa_S\ \alpha_\phi^{(1)} - N\sin\theta_0\ \delta y_2 \\ e_6 & = & \kappa_S\ \delta y_1 - \kappa_N\ \delta y_2. \end{array}$$

With respect to the resulting basis for $\mathcal{N}$, the Hessian $\mathsf{d}^2 H_\xi|_{\mathcal{N}}(x_e)$ block diagonalizes into two 3×3 blocks (for the $\ell = 1$ mode) and the remainder is diagonal, while $L_{\mathcal{N}}$ block diagonalizes into one 6×6 block (for $\ell = 2$), and the remainder into 2×2 blocks.

If $\mu = 0$ and $n \geq 3$ one can take for example $\{e_2, e_3, e_5, e_6\}$ as a basis for V_1.

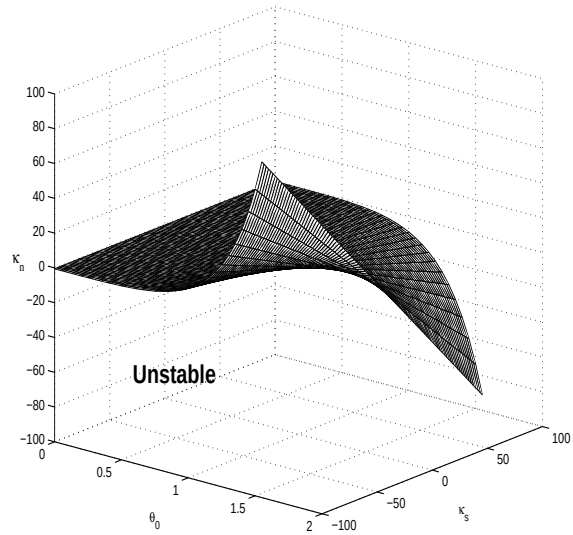

FIGURE 9.1. The relative equilibria $\mathbf{C}_{nv}(R, 2p)$ in the Northern hemisphere are unstable 'below' this ruled surface in $(\theta_0, \kappa_S, \kappa_N)$-space, shown in the figure for $n = 4$. Above the surface the relative equilibrium is stable with respect to all the $\ell \geq 2$ modes.

Proof. The proof is similar to that for a single ring (see Section 3.2 and Proposition 5.1). □

9.1. **The higher modes $\ell \geq 2$.** The mode $\ell = 1$ gives a 3×3 block (for $\mu \neq 0$ and $n > 2$) from which, unfortunately, we can not derive a useful formula for stability analogous to that for a single polar vortex. However, we can derive formulae for the stability of the other modes, and thereby obtain the following sufficient condition for instability, illustrated by Figures 9.1 and 9.2. These modes occur (with the same bases) for $\mu = 0$ and $\mu \neq 0$ and the results here are valid in both cases, but only for $n \geq 4$: for $n = 2, 3$ the only mode is $\ell = 1$.

Theorem 9.2. *A $\mathbf{C}_{nv}(R, 2p)$ relative equilibrium with $n \geq 4$ and $\mu \neq 0$ is linearly unstable if*

$$\kappa_N(1 + \cos\theta_0)^2 + \kappa_S(1 - \cos\theta_0)^2 < \left[\frac{n^2}{4}\right] - (n-1)(1 + \cos^2\theta_0),$$

and is stable with respect to the $\ell \geq 2$ modes if this inequality is reversed.

Thus one finds increasing either polar vorticity tends to stabilize the relative equilibrium, and if both polar vorticities are negative then the system is linearly unstable (this is only for $n \geq 4$).

Proof. The proof is similar to that for Theorem 6.2. Following the notation of the proof of that theorem, we have that the eigenvalues of the reduced Hessian are given by $\lambda_\phi^{(\ell)} = n\ell(n - \ell)/2$ and

$$\lambda_\theta^{(\ell)} = \frac{n}{2\sin^2\theta_0}\left[-(\ell-1)(n-\ell-1)+(n-1)\cos^2\theta_0+\kappa_N(1+\cos\theta_0)^2 \right.$$
$$\left. +\kappa_S(1-\cos\theta_0)^2\right].$$

The relative equilibrium is linearly unstable if there exists $\ell \geq 2$, such that $\lambda_\theta^{(\ell)} < 0$. Since the least $\lambda_\theta^{(\ell)}$ is for $\ell = [n/2]$, the relative equilibrium is linearly unstable if

$$-([n/2]-1)(n-[n/2]-1)+(n-1)\cos^2\theta_0+\kappa_N(1+\cos\theta_0)^2+\kappa_S(1-\cos\theta_0)^2 < 0,$$

and is stable with respect to the $\ell \geq 2$ modes if this inequality is reversed. This gives the desired criterion. □

Stability of the $\ell \geq 2$ modes From the theorem we can deduce the following results about the (in)stability of the $\mathbf{C}_{nv}(R, 2p)$ relative equilibria with respect to the $\ell \geq 2$ modes. These modes only occur for $n \geq 4$. We continue to assume the ring lies in the Northern hemisphere.

- In the limiting case as the ring converges to the North pole ($\theta_0 = 0$), for all values of κ_S the relative equilibria are linearly unstable if $\kappa_N < \frac{1}{4}(\left[n^2/4\right] - 2n+2)$. This agrees with the instability of a ring and single pole when '$\kappa < \kappa_0$' in Proposition 6.2.
- At the opposite extreme, when the ring is at the equator ($\theta_0 = \pi/2$) they are linearly unstable if $\kappa_N + \kappa_S < \left[n^2/4\right] - n + 1$. The right hand side of this inequality is non-negative for all positive integers n, and so the 'equatorial' $\mathbf{C}_{nv}(R, 2p)$ relative equilibria are unstable if the total polar vorticity has opposite sign to that of the ring. If $\kappa_N + \kappa_S > 0$ then the critical ratio of the total polar vorticity to the total ring vorticity needed to stabilize the $\ell \geq 2$ modes grows linearly with n.
- For all $n \geq 4$ the relative equilibria are unstable for all latitudes in the Northern hemisphere if $\kappa_N < \frac{1}{4}(\left[n^2/4\right] - 2n+2)$ *and* $\kappa_N + \kappa_S < \left[n^2/4\right] - n + 1$. In particular, for $n \geq 7$ the relative equilibria are unstable for all θ_0 if $\kappa_N < 0$ and $\kappa_S < 0$.

To determine which of these relative equilibria that are stable to the higher modes, are in fact *genuinely stable* RE it is necessary to evaluate the eigenvalues arising from the $\ell = 1$ mode. This we do numerically except in the special case of an equatorial configuration with polar vortices of equal strength.

9.2. **Numerical study of the mode $\ell = 1$.** For $n > 2$ and $\mu \neq 0$ the subspace V_1 is 6-dimensional, with basis given in Proposition 9.1. We are only able to obtain analytical results in the special case that the configuration is an equatorial RE with zero momentum. In other cases we have performed a numerical study using MAPLE. In this numerical study, we only investigate the 'possibly stable' regime given by Theorem 9.2; that is, we assume, for $n > 3$, that

$$\kappa_N(1+\cos\theta_0)^2+\kappa_S(1-\cos\theta_0)^2 > \left[\tfrac{n^2}{4}\right] - (n-1)(1+\cos^2\theta_0).$$

For $n = 2$ and 3 there is no higher mode. There are many details here that invite further investigation. The case $n = 2$ is rather different from the others, and we treat it in a separate section. The principal difference between $n = 3$ and $n > 3$ is the presence or not of higher modes. We show the figures for $n = 3$ in some detail (see Figure 9.3). The figures for $n > 3$ are similar (after a rescaling of the polar

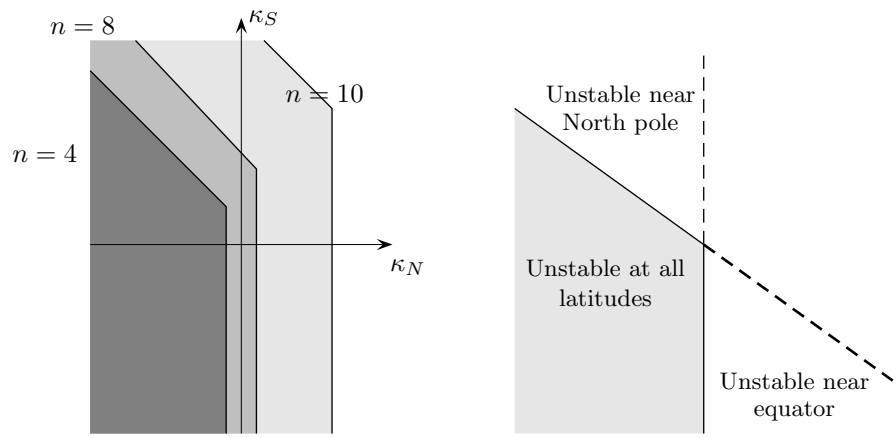

FIGURE 9.2. Schematic diagram showing the instabilities of the $\mathbf{C}_{nv}(R, 2p)$ configurations due to the $\ell \geq 2$ modes: (a) The shaded regions depict the values of the polar vorticities for which *all* the relative equilibria in the Northern hemisphere are unstable: the darkest region represents $n = 4$, the next $n = 8$ and the lightest $n = 10$. (b) demonstrates that above each shaded region of (a) the corresponding relative equilibria near the North pole are unstable, while to the right it is the relative equilibria near the equator which are unstable.

vorticities), but have a cut-off given by the higher modes. Figure 9.4 shows the case $n = 4$.

Equatorial RE *with zero momentum* The configuration with an equatorial ring ($\theta_0 = \pi/2$) has momentum zero when $\kappa_S = \kappa_N$ ($= \kappa$). Since in this case the relative equilibrium is in fact an equilibrium, a method for the full analysis of the relative equilibria in a neighbourhood can be found in [28], particularly Theorems 2.1 and 2.7. The fact that the symmetry group of the relative equilibrium is $\mathbf{D}_n \times \mathbb{Z}_2$ (where $\mathbb{Z}_2$ is reflexion in the equator, which acts antisymplectically, as in [28]), the results of that paper show that, assuming generic higher order terms, for each μ close to zero there are (generically) $2n + 2$ relative equilibria, two of which have $\mathbf{D}_n$ symmetry and these are the points which lie on the $\mathbf{C}_{nv}(R, 2p)$-stratum we are considering. If the equatorial RE is Lyapounov stable (see below), then the two nearby ones on this stratum can be either elliptic or Lyapounov stable depending on higher order terms (and we see from the numerics they are elliptic).

For this zero-momentum equatorial equilibrium, the $\ell = 1$-mode is just 4-dimensional (for $n > 2$), and can be spanned by the basis $\{e_2, e_3, e_5, e_6\}$ from the proposition above. The Hessian on this mode block diagonalizes as two identical 2x2 matrices.

Proposition 9.3. *For $n \geq 3$, the eigenvalues of the linear system at the equilibrium with zero momentum on the equator are*

$$\lambda = \pm\tfrac{1}{2}\sqrt{-n^2 - 2\kappa(n-4)}\,.$$

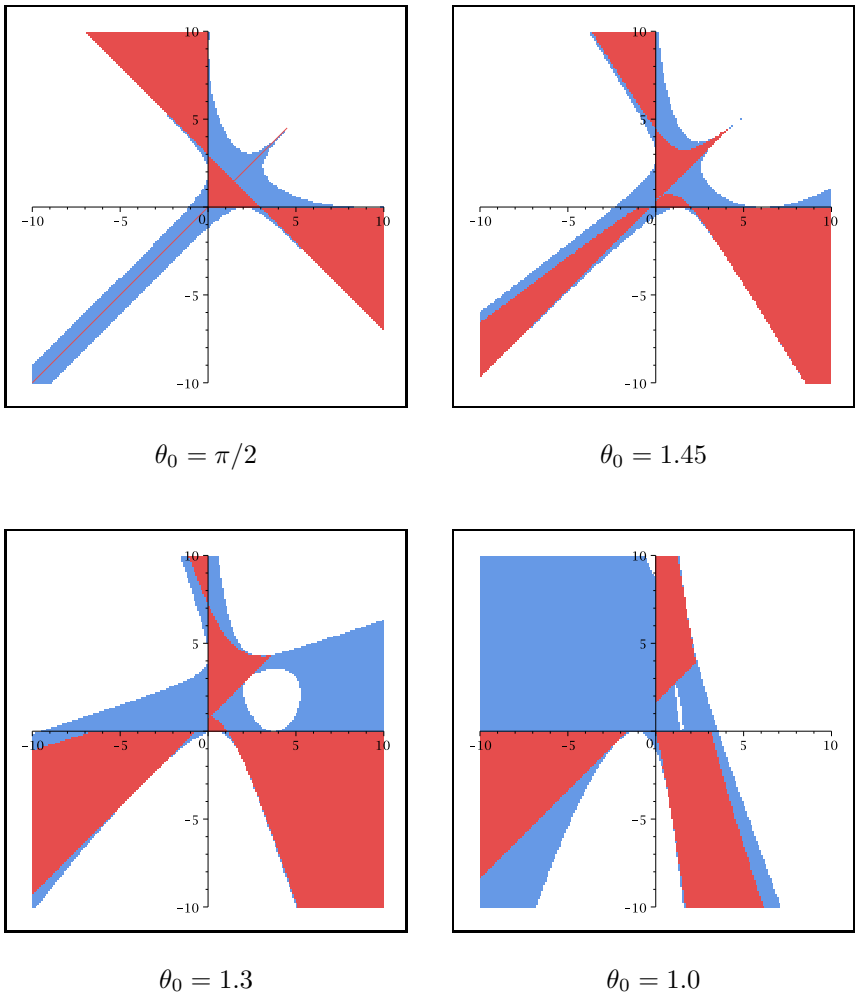

FIGURE 9.3. Stability diagrams for a 3-ring with two polar vortices — $\mathbf{C}_{3v}(R, 2p)$, showing vorticities in the range $|\kappa_N|$, $|\kappa_S| \leq 10$, at four specific values of the co-latitude. The horizontal axis is κ_N, the vertical κ_S. See Fig. 6.2 for the meaning of the colours.

In particular, combining with the higher modes when $n > 3$, we deduce that this configuration is Lyapounov stable under the following circumstances:

$n = 3$	$n = 4$	$n = 5$	$n = 6$	$\dots$	$n = 12$
$\kappa < \frac{9}{2}$	$\kappa > \frac{1}{2}$	$\kappa > 1$	$\kappa > 4$		$\kappa > \frac{25}{2}$

If the inequality is reversed, the configuration is linearly unstable.

Other configurations For these we have not succeeded in obtaining analytic conditions. The numerical calculations suggest the following:

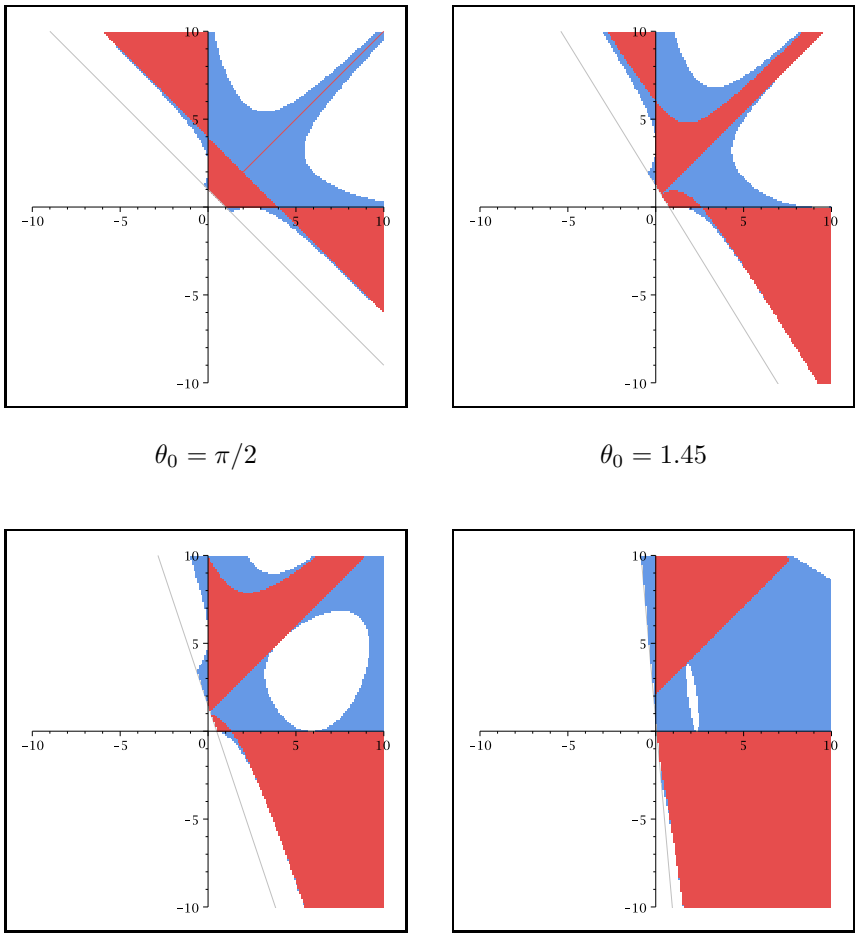

FIGURE 9.4. Stability diagrams for a 4-ring with 2 poles (that is, $\mathbf{C}_{4v}(R, 2p)$), showing vorticities in the range $|\kappa_N|$, $|\kappa_S| \leq 10$, at four specific values of the co-latitude. Below and to the left of the grey line the configuration is unstable to the higher modes. The horizontal axis is κ_N, the vertical κ_S. The stability diagrams for $n > 4$ are all similar (after a change in the scale of the vorticity). See Fig. 6.2 for the meaning of the colours.

- For all n and for all sufficiently large and positive polar vorticities there are ranges of θ_0 with elliptic relative equilibria.
- For all n and for κ_N sufficiently positive and $\kappa_S < 0$ there are Lyapounov stable relative equilibria with the ring in the Northern hemisphere.
- When the equatorial ring configuration has non-zero momentum, one finds several regions of stability, shown in the first plot in each of Figures 9.3 and 9.4. In particular the reduced Hessian is degenerate if $\kappa_N + \kappa_S = n$.

- The straight line between the Lyapounov and elliptic regions in the two figures is where $\mu = 0$.
- The transition between elliptic and unstable in the upper right hand part of the diagram is through a Hamiltonian Hopf bifurcation.
- The point where the unstable region is tangent to the line $\mu = 0$ (most visible for $\theta_0 = 1.3$) arises where there is a ro-vibrational resonance, as described in Section 4.3. The transitions between elliptic and unstable RE arbitrarily close to this point arise as Hamiltonian Hopf bifurcations, a fact which resonates with the description in [25].

9.3. **Kite configurations: $\mathbf{C}_{2v}(R, 2p)$.** Here we consider the remaining case $n = 2$, which consists of a 2-ring with two poles: this is a kite-shaped configuration of vortices lying on a meridian, where the meridian rotates in time about the axis through the poles. The only mode in the symplectic slice is $\ell = 1$, which is 4-dimensional, or 2-dimensional when $\mu = 0$. It has a basis

$$\begin{aligned} e_1 &= \kappa_N\, \alpha_\theta^{(1)} - 2\cos\theta_0\, \delta x_1\,, & e_2 &= \kappa_S\, \delta x_1 - \kappa_N\, \delta x_2 \\ e_3 &= \kappa_N\, \alpha_\phi^{(1)} - 2\sin\theta_0\, \delta y_1, & e_4 &= \kappa_S\, \delta y_1 - \kappa_N\, \delta y_2\,. \end{aligned}$$

The subspaces $\langle e_1, e_2\rangle$ and $\langle e_3, e_4\rangle$ are both Lagrangian and invariant under the group. The reflexion $\kappa : (x, y, z) \to (x, -y, z)$ acts trivially on the first of these subspaces and by $-I$ on the second, which implies that the Hessian on this slice block diagonalizes. The entries are too long to usefully reproduce here.

When $\mu = 0$, the symplectic slice is 2-dimensional, and we can use $\{e_1, e_3\}$ as a basis. Because of the invariance under the reflexion κ, the reduced Hessian on this slice is a diagonal matrix, but again one obtains expressions too long to usefully reproduce here. In the special case of an equatorial configuration, which has momentum zero if and only if $\kappa_N = \kappa_S$ $(= \kappa)$, the diagonal Hessian simplifies to $\mathrm{diag}[4\kappa^3, -4\kappa^2]$, so the configuration is Lyapounov stable if $\kappa < 0$ and linearly unstable if $\kappa > 0$.

The angular velocity of the relative equilibrium is given by

$$\xi = \frac{1}{\sin^2\theta_0}\left((\kappa_N + \kappa_S + 1)\cos\theta_0 + \kappa_N - \kappa_S\right).$$

Conclusions from numerics See Figure 9.5. Note that with just 4 vortices, the reduced spaces have dimension 4, so any elliptic (relative) equilibria has a good chance of being Lyapounov stable, by KAM confinement. We have not checked any of the non-degeneracy conditions for this to hold, so we continue to distinguish between RE that we know to be Lyapounov stable by energy-momentum confinement (definiteness of the Hessian on the symplectic slice), and those we only know to be elliptic.

- If both polar vorticities are positive then all configurations are linearly unstable.
- Apart from a very small region, the only Lyapounov stable configurations occur with both polar vorticities negative. The very small region has $\kappa_S > 0$ but small, and $\kappa_N < 0$ (for the ring in the Northern hemisphere); it is close to the line where $\mu = 0$.
- If the ring is equatorial ($\theta_0 = \pi/2$), so the configuration is a square lying on a great circle, with one pair of opposite vortices having unit vorticity, and the other two having vorticity κ_N and κ_S, one sees that the relative equilibrium

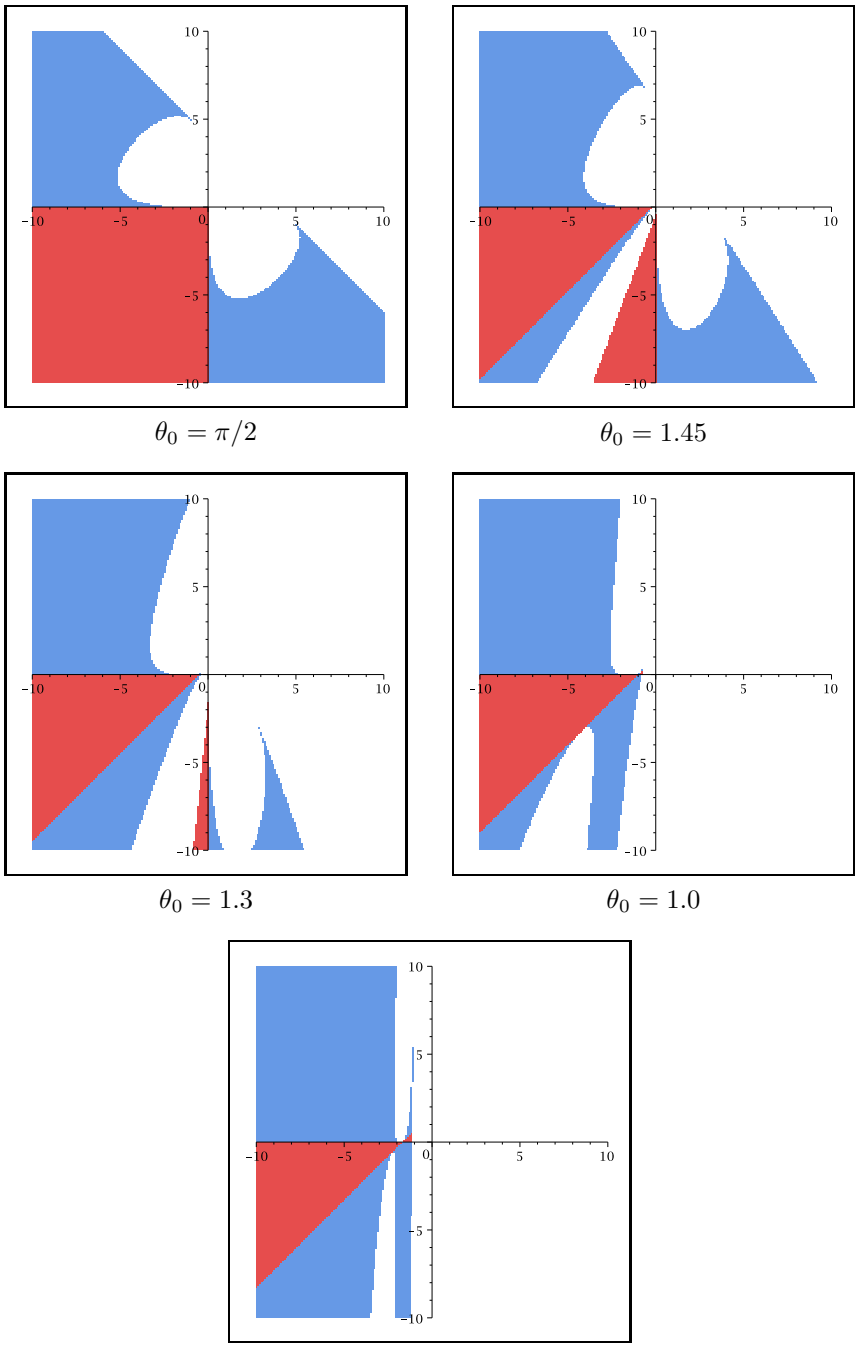

FIGURE 9.5. Stability diagrams for the kite-shaped configuration $\mathbf{C}_{2v}(R, 2p)$. Showing $|\kappa_N|$, $|\kappa_S| \leq 10$, at five specific values of the co-latitude. The horizontal axis is κ_N, the vertical κ_S. See Fig. 6.2 for the meaning of the colours.

is Lyapounov stable if and only if both $\kappa_N, \kappa_S < 0$. There is a transition across the line $\kappa_N + \kappa_S = 4$, to the right of which the system has a pair of real eigenvalues and a pair of imaginary ones. In the unstable 'bulbs' near the origin, the linear system has a quadruplet of eigenvalues, and the transition from the nearby elliptic regions is via a Hamiltonian Hopf bifurcation..

- As the ring is placed nearer the North pole, there opens up a region of instability near the negative part of the diagonal. The straight line boundary between the Lyapounov stable and elliptic regions corresponds to $\mu = 0$ (here we have $\mu = \kappa_N - \kappa_S + 2\cos\theta_0$), and so the transition is that described in Section 4.3. The transition from elliptic to unstable is through a pitchfork of splitting type, giving a pair of imaginary and a pair of real eigenvalues. Continuing the path to the right, the two real eigenvalues meet again at 0 to become imaginary, giving a Lyapounov stable configuration via another pitchfork of splitting type.
- There is a point of interest on the $\mu = 0$ locus (particularly visible in the figure for $\theta_0 = 1.0$) where the region of linear stability (in white) is tangent to the region of Lyapounov stability (in red). This occurs at points where there is a ro-vibrational resonance, as described in Section 4.3.
- In the region of linear instability shown in the bottom left quadrant of the $\theta_0 = 1.0$ diagram (in the $\theta_0 = 1.3$ diagram the corresponding region would be further out, and so is not seen), the linear system has a quadruplet of eigenvalues, and the transition from the elliptic region into this unstable one is by a Hamiltonian Hopf bifurcation, corresponding to the fact that the ro-vibrational resonance of the previous point is essentially a form of Hamiltonian-Hopf bifurcation.

REFERENCES

[1] H. Aref, P. Newton, M. Stremler, T. Tokieda and D. L. Vainchtein, *Vortex crystals*. Adv. Appl. Mech., **39** (2003), 1–79.

[2] V. Bogomolov, *Dynamics of vorticity at a sphere*, Fluid Dyn., **6** (1977), 863–870.

[3] S. Boatto and H. E. Cabral, *Nonlinear stability of a latitudinal ring of point-vortices on a nonrotating sphere*, SIAM J. Appl. Math., **64** (2003), 216–230.

[4] P.-L. Buono, F. Laurent-Polz and J. Montaldi, *Symmetric Hamiltonian Bifurcations*, in "Geometric Mechanics and Symmetry," Based on lectures by Montaldi, LMS Lecture Note Series, **306**, Cambridge University Press, Cambridge, (2005), 357–402.

[5] H. E. Cabral, K. R. Meyer and D. S. Schmidt, *Stability and bifurcations for the $N+1$ vortex problem on the sphere*, Regular and Chaotic Dynamics, **8** (2003), 259–282.

[6] H. E. Cabral and D. S. Schmidt, *Stability of relative equilibria in the problem of $N+1$ vortices,* SIAM J. Math. Anal., **31** (1999/00), 231–250.

[7] P. Chossat, J.-P. Ortega and T. Ratiu, *Hamiltonian Hopf bifurcation with symmetry*, Arch. Ration. Mech. Anal., **163** (2002), 1–33. *Correction to "Hamiltonian Hopf bifurcation with symmetry"*, Arch. Ration. Mech. Anal., **167** (2002), 83–84.

[8] G. Derks and T. Ratiu, *Unstable manifolds of relative equilibria in Hamiltonian systems with dissipation*, Nonlinearity, **15** (2002), 531–549.

[9] M. Golubitsky and I. Stewart, *Generic bifurcation of Hamiltonian systems with symmetry*, With an appendix by Jerrold Marsden, Physica D, **24** (1987), 391–405.

[10] H. Helmholtz, *Über Integrale der hydrodynamischen Gleichungen welche den Wirbelbewegungen entsprechen*, Crelles J., **55** (1858), 25–55. English translation, *On integrals of the hydrodynamical equations which express vortex motion*, Phil. Mag., **33** (1867), 485–512.

[11] E. Hansen, "A Table of Series and Products," Prentice-Hall, 1975.

[12] R. Kidambi and P. Newton, *Motion of three point vortices on a sphere*, Physica D, **116** (1998), 143–175.

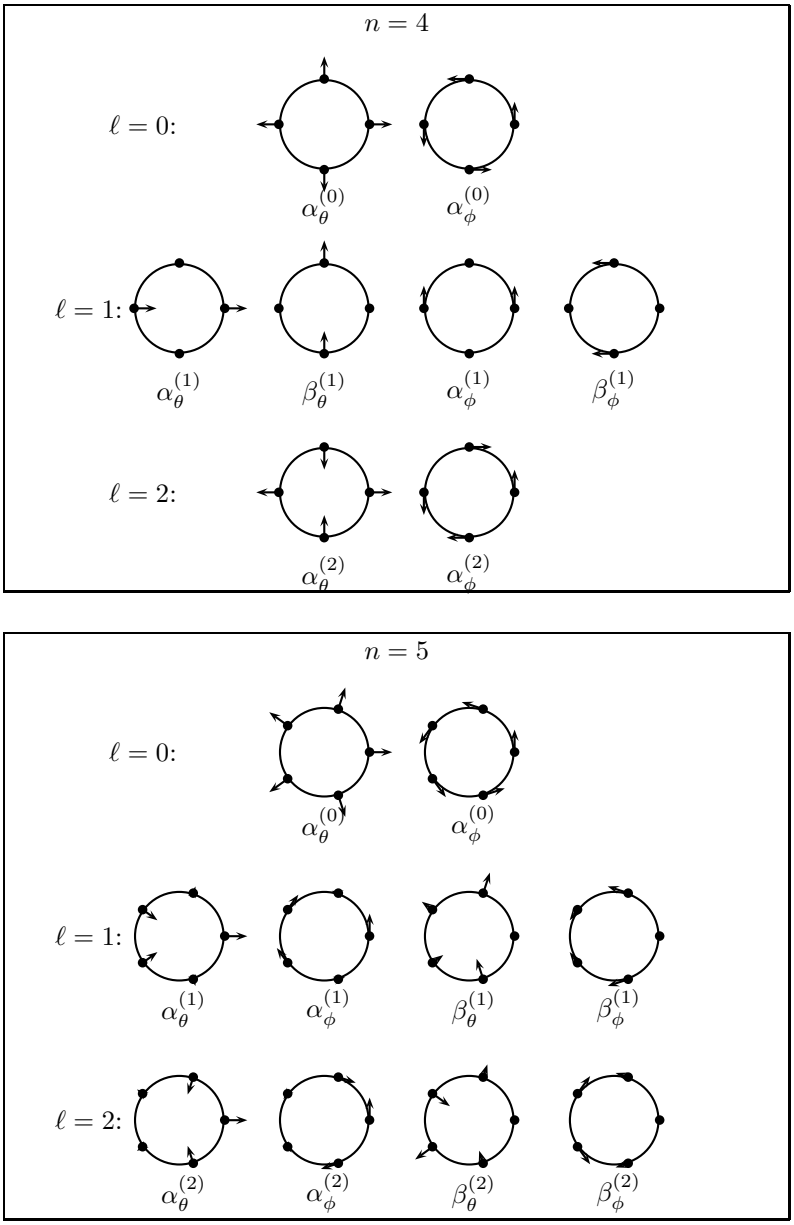

FIGURE 9.6. The *Fourier bases* for rings of type R with $n = 4$ and 5 points.

[13] G. Kirchhoff, "Vorlesungen über Mathematische Physik, Mechanik," Kap. XX, Teubner, Leipzig, 1876.

[14] L. G. Kurakin, *On the nonlinear stability of the regular vortex systems on a sphere*, Chaos, **14** (2004), 592–602.

[15] F. Laurent-Polz, *Point vortices on the sphere: A case with opposite vorticities*, Nonlinearity, **15** (2002), 143–171.

[16] F. Laurent-Polz, *Relative periodic orbits in point vortex systems*, Nonlinearity, **17** (2004), 1989–2013.

[17] F. Laurent-Polz, *Point vortices on a rotating sphere*, Regul. Chaotic Dyn., **10** (2005), 39–58.
[18] F. Laurent-Polz, "Etude Géométrique de la Dynamique de N Tourbillons Ponctuels sur une Sphère," Ph.D Thesis, University of Nice, 2002.
[19] C. Lim, J. Montaldi and M. Roberts, *Relative equilibria of point vortices on the sphere*, Physica D, **148** (2001), 97–135.
[20] J. Marsden, S. Pekarsky and S. Shkoller, *Stability of relative equilibria of point vortices on a sphere and symplectic integrators*, Nuovo Cimento C, **22** (1999), 793–802.
[21] J.-C. van der Meer, "The Hamiltonian Hopf Bifurcation," Lecture Notes in Mathematics, **1160**, Springer-Verlag, Berlin, 1985.
[22] G. J. Mertz, *Stability of body-centered polygonal configurations of ideal vortices*, Phys. Fluids, **21** (1978), 1092–1095.
[23] K. R. Meyer and D. S. Schmidt, *Periodic orbits near L4 for mass ratios near the critical mass ratio of Routh*, Celest. Mech., **4** (1971), 99–109.
[24] K. R. Meyer and D. S. Schmidt, *Bifurcations of relative equilibria in the N-body and Kirchhoff problems*, SIAM J. Math. Anal., **19** (1988), 1295–1313.
[25] J. Montaldi, *Persistence and stability of relative equilibria*, Nonlinearity, **10** (1997), 449–466.
[26] J. Montaldi, *Bifurcations of relative equilibria near zero momentum in* $\mathsf{SO}(3)$*-symmetric Hamiltonian systems*, in preparation.
[27] J. Montaldi, Web pages, http://www.maths.manchester.ac.uk/jm/Vortices
[28] J. Montaldi and M. Roberts, *Relative equilibria of molecules*, J. Nonlinear Sci., **9** (1999), 53–88.
[29] J. Montaldi, M. Roberts and I. Stewart, *Periodic solutions near equilibria of symmetric Hamiltonian systems*, Phil. Trans. R. Soc. London Ser. A, **325** (1988), 237–293.
[30] J. Montaldi, M. Roberts and I. Stewart, *Existence of nonlinear normal modes of symmetric Hamiltonian systems*, Nonlinearity, **3** (1990), 695–730.
[31] J. Montaldi, A. Soulière and T. Tokieda, *Vortex dynamics on a cylinder*, SIAM J. on Applied Dynamical Systems, **2** (2003), 417–430.
[32] J. Montaldi and T. Tokieda, *A family of point vortex systems*, in preparation.
[33] P. Newton, "The N-Vortex Problem. Analytical Techniques," Applied Mathematical Sciences, **145**, Springer-Verlag, New York, 2001.
[34] J.-P. Ortega, "Symmetry, Reduction, and Stability in Hamiltonian Systems," Ph.D Thesis, University of California, Santa Cruz, 1998.
[35] R. Palais, *Principle of symmetric criticality*, Comm. Math. Phys., **69** (1979), 19–30.
[36] G. Patrick, *Relative equilibria in Hamiltonian systems: The dynamic interpretation of nonlinear stability on a reduced phase space*, J. Geom. Phys., **9** (1992), 111–119.
[37] G. Patrick, *Dynamics near relative equilibria: Nongeneric momenta at a 1:1 group-reduced resonance*, Math. Z., **232** (1999), 747–788.
[38] L. Polvani and D. Dritschel, *Wave and vortex dynamics on the surface of a sphere*, J. Fluid Mech., **255** (1993), 35–64.
[39] S. Pekarsky and J. Marsden, *Point vortices on a sphere: Stability of relative equilibria*, J. Math. Phys., **39** (1998), 5894–5907.
[40] J.-P. Serre, "Représentations Linéaires des Groupes Finis," Third revised edition, Hermann, Paris, 1978.
[41] A. Soulière and T. Tokieda, *Periodic motions of vortices on surfaces with symmetry*, J. Fluid Mech., **460** (2002), 83–92.
[42] T. Tokieda, *Tourbillons dansants*, C.R. Acad. Sci. Paris Série I Math., **333** (2001), 943–946.

Received March 2011; revised May 2011.

E-mail address: laurentpolzfj@voila.fr
E-mail address: j.montaldi@manchester.ac.uk
E-mail address: m.roberts@surrey.ac.uk